Asmaa Abbas, Ranjit K. Prajapati, Emil Aalto-Setälä, Alexander A. Baykov, Anssi M. Malinen; Aflatoxin biosynthesis regulators AflR and AflS: DNA binding affinity, stoichiometry, and kinetics. Biochem J 20 June 2024; 481 (12): 805–821. doi: https://doi.org/10.1042/BCJ20240084

Title
Aflatoxin biosynthesis regulators AflR and AflS: DNA binding affinity, stoichiometry, and kinetics

Authors
Asmaa Abbas[1], Ranjit K. Prajapati[1], Emil Aalto-Setälä[1], Alexander A. Baykov[2], Anssi M. Malinen[1]

Affiliations
[1] Department of Life Technologies, University of Turku, Turku, Finland
[2] Belozersky Institute of Physico-Chemical Biology, Lomonosov Moscow State University, Moscow, Russia.

Corresponding author information
Anssi Malinen
Department of Life Technologies
20014 University of Turku
Finland
anssi.malinen@utu.fi
tel. +358 50 4364 100

Abstract
Aflatoxins, potent foodborne carcinogens produced by *Aspergillus* fungi, pose significant health risks worldwide and present challenges to food safety and productivity in the food chain. Novel strategies for disrupting aflatoxin production, cultivating resilient crops, and detecting contaminated food are urgently needed. Understanding the regulatory mechanisms of aflatoxin production is pivotal for targeted interventions to mitigate toxin accumulation in food and feed. The gene cluster responsible for aflatoxin biosynthesis encodes biosynthetic enzymes and pathway-specific regulators, notably AflR and AflS. While AflR, a DNA-binding protein, activates gene transcription within the cluster, AflS enhances aflatoxin production through mechanisms that are not fully understood. In this study, we developed protocols to purify recombinant AflR and AflS proteins and utilised multiple assays to characterize their interactions with DNA. Our biophysical analysis indicated that AflR and AflS form a complex. AflS exhibited no DNA binding capability on its own but unexpectedly reduced the DNA binding affinity of AflR. Additionally, we found that AflR achieves its binding specificity through a mechanism in which either two copies of AflR or its complex with AflS bind to target sites on DNA in a highly cooperative manner. The estimated values of the interaction parameters of AflR, AflS and DNA target sites constitute a fundamental framework against which the function and mechanisms of other aflatoxin biosynthesis regulators can be compared.

Keywords
aflatoxin; transcription factor; AflR; AflS; DNA binding

Abbreviations: AFs, aflatoxins; *A. flavus*, *Aspergillus flavus*; EMSA, electrophoretic mobility shift assay; IMAC, immobilized metal affinity chromatography; SEC, size-exclusion chromatography; MST, microscale thermophoresis; PIFE, protein induced fluorescence enhancement; SF, stopped flow; RSS, residual sum of square; MBP, maltose binding protein; LB, Luria Broth media.

Introduction

Aflatoxins (AFs) are a group of hazardous secondary metabolites produced by fungi, specifically *Aspergillus flavus* and *Aspergillus parasiticus*. AFs are well-known for their potent carcinogenicity and can cause both acute poisoning and chronic diseases **[1]**. The gene cluster encoding the biosynthesis pathway of AFs includes at least 30 genes, which span an 80-kb region in the genome of AF-producing *Aspergillus* strains. The expression of biosynthesis enzyme genes is controlled by positive and negative global regulators and by two pathway-specific activators, AflR and AflS **[2]**. AflR is crucial for the transcriptional activation of most genes in the AF biosynthetic pathway **[3]**. The deletion of *aflR* caused drastic reduction in AFs production, with the residual level of aflatoxin B1 dropping in two independent studies either below the detection limit **[2]** or to 0.1% of that in the wild-type strain **[3]**. Conversely, the overexpression of *aflR* in *A. flavus* resulted in increased transcript levels of AF pathway genes and AFs accumulation **[4]**. AflR also appears to have a broader regulator role in the growth and development of *A. flavus* because Δ*aflR* strain was rendered incapable of producing conidia or asexual propagules **[3]**. Additionally, broad changes in the expression levels of the genes involved in spore germination, sclerotial development, and carbohydrate metabolism were observed **[3]**.

AflR is a 47-kDa protein containing a GAL4-type binuclear zinc finger $Zn(II)_2(Cys)_6$ cluster responsible for DNA-binding activity near the N-terminus **[5,6]** and an acidic transcription activation domain near the C-terminus **[7]**. AflR binds tightly, based on the results of *in vitro* electrophoretic mobility shift assay (EMSA) and footprinting, to the specific recognition sequence, 5'-$TCGN_5CGA$-3', in the promoters of AF biosynthesis genes **[8,9]**. The symmetry of the two sequence-specific base triplets and the preference for a linker length of five base pairs between them imply that the sequence may be bound by two AflR molecules, similar to yeast GAL4 in complex with its target DNA **[10]**. However, the binding specificity of AflR is not absolutely restricted to the above sequence. Analysis of more diverse sequences has defined a more general consensus binding motif as 5′-TCGSWNNSCGR-3′ (W=A or T, S=G or C, R=A or G) **[9]**. Most of these putative AflR binding sites locate 100–200-bp upstream from the translation start site but are also frequently present further upstream in the promoter **[11]**. ChIP-seq based *in vivo* mapping of AflR binding sites in *A. flavus* defined a longer consensus motif (18 bp vs 11 bp) as 5′-CSSGGGWTCGAWCCCSSG-3′, which may encode two adjacent AflR-binding sites in the top and bottom DNA strands, respectively **[12]**. However, because all detected binding events are located outside the AF gene cluster, *A. flavus* was probably not expressing genes of the AF cluster or producing AF under the conditions used.

The AF biosynthesis gene cluster includes another pathway-specific regulator gene, *aflS* (formerly known as *aflJ*), adjacent to *aflR* and transcribed in the opposite direction **[13]**. The detailed mechanism of AflS function remains incompletely understood, but it consistently appears to amplify the activating effect of AflR on AF biosynthesis. However, in most studies, AflS was neither essential for AF biosynthesis nor able to rescue AF production in the absence of AflR (reviews **[11,14,15]**). A yeast two-hybrid assay suggested protein-protein interaction between AflS and AflR, potentially indicating that AflS directly modulates, as a co-activator, the transcription factor function of AflR **[16,17]**. Consistent with synergistic function, *A. parasiticus* strains transformed with both *aflR* and *aflS* genes produced higher amounts of AF precursors compared to strains transformed with *aflR* alone **[18]**. At the transcriptional level, AflS was found to promote the expression-specific AF pathway genes rather than exerting universal effects **[13,17,19]**. The absence of AflS enrichment on known AflR binding sites in chromatin immunoprecipitation (ChIP) experiments, coupled with fluorescence microscopy-based evidence of AflR·AflS complex formation in the aflatoxisomes/endosomes, has led to an alternative hypothesis. According to it, AflS functions as a chaperone-like protein, promoting AflR transport to the nucleus and aflatoxin secretion **[17]**.

In this study, we set to investigate the molecular mechanism underlying the DNA binding activity of AflR and its potential modulation by AflS. To this end, we developed protocols to purify recombinant AflR and AflS proteins and used biophysical approaches to characterize the interactions between them and their interaction with target DNA. The biophysical data showed that AflR and AflS form a stable complex and defined the pathways and stoichiometry of their binding to DNA, providing molecular insights into their regulatory function in aflatoxin biogenesis.

Results

Production and purification of AflR and AflS

Highly purified recombinant AflR and AflS proteins were initially obtained for studying their interactions with each other and with DNA. To achieve this, we inserted synthetic codon-optimized genes into pET-21(+)-based expression vectors with an inducible T7 promoter. These constructs for both proteins also encoded an N-terminal His-tag to facilitate protein purification. Initially, the *aflR* expression plasmid (pAM068) **(Fig. 1A)** was transformed into the *Escherichia coli* strain T7 Express, but the resulting recombinant protein accumulated, after a 3 h-expression at 37°C, predominantly in cell lysate pellet, likely as inclusion bodies **(Fig. S1A)**. To avoid AflR precipitation, we transformed pAM068 into *E. coli* strain BL21 (DE3) and induced the expression culture overnight at reduced temperature (16°C) and shaking speed (160 rpm). Successful overexpression of AflR in a soluble form was achieved following this modified protocol.

The recombinant AflR was purified from the cell lysate supernatant using a combination of immobilized metal affinity chromatography (IMAC) and size-exclusion chromatography (SEC) **(Fig. 1A)**. SDS-PAGE analysis of the obtained protein preparation revealed a major band with a molecular mass of approximately 50-kDa, corresponding to the calculated mass of AflR **(Fig. 1A)**. Western blot analysis using anti-His-tag antibody further confirmed the identity of the purified AflR **(Fig. 1A)**. The typical purification yield was about 2 mg of AflR from 6 L of bacterial culture.

The AflS protein could not be produced from the pAM069 plasmid in a soluble form under various conditions. To enhance solubility, we added His-tagged maltose binding protein (MBP) to the N-terminal end of AflS. The resulting fusion protein, henceforth referred to as AflS(MBP), was produced in a soluble form from the plasmid pAM073 **(Fig. 1B)** in *E. coli* BL21(DE3) and purified using ammonium sulfate precipitation, IMAC, anion exchange and dextrin affinity chromatography (MBPTrap) **(Fig. 1B)**. The SDS-PAGE mobility of the purified AflS(MBP) corresponded to its calculated molecular mass (90 kDa) **(Fig. 1B)**. Western blot analysis with an anti-His-tag antibody further confirmed the identity of the purified AflS(MBP). Typical purification yield was 2 mg of protein from 2 L of bacterial culture.

Importantly, the removal of the MBP tag from purified AflS(MBP) by site-specific TEV protease led to AflS precipitation, indicating the importance of MBP for solubility **(Fig. S1B)**. Because it was impossible to remove MBP from AflS(MBP), we separately produced and purified the MBP protein **(Fig. 1C)**, using the plasmid pAM074, to serve as a negative control in the functional assays. A two-step purification procedure, consisting of ammonium sulfate precipitation and MBPTrap **(Fig. 1C)**, typically yielded 9 mg MBP protein from 2 L of bacterial culture **(Fig. 1C)**.

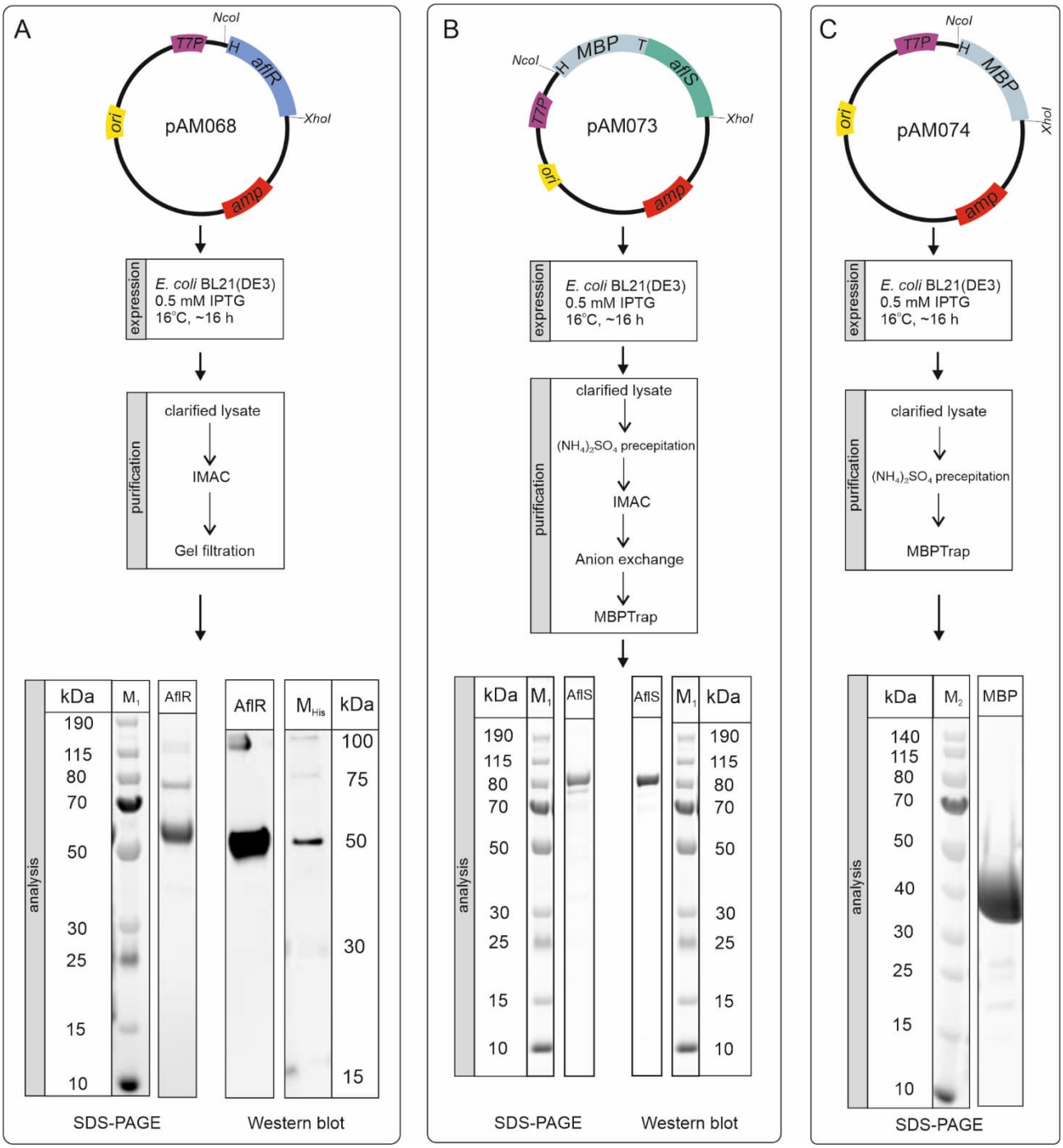

Figure 1. Expression, purification and analysis of recombinant proteins. (A), AflR; (B), MBP-tagged AflS; (C), MBP. Protein encoding genes were inserted between *NcoI* and *XhoI* restriction sites in pET21-based vector, which provided the final construct with T7 RNA polymerase promoter (*T7P*), ColE1-type origin of replication (*ori*) and ampicillin resistance marker (*amp*). The positions of hexa-histidine tag and TEV protease cleavage sites are indicated with H and T, respectively. The purified proteins were analysed by SDS-PAGE (Coomassie staining) and Western blotting (anti-His-tag antibody). Gel lanes labeled with M_1, M_2 and M_{His} represent protein ladders with indicated molecular masses (M_1, PageRuler^{TM} Plus prestained protein ladder, ThermoFisher Scientific; M_2, PageRuler^{TM} prestained protein ladder, ThermoFisher Scientific; M_{His}, 6xHis Protein Ladder, Qiagen). The pairs of sample and marker gel slices are from the same gel/blot.

AflS interacts with AflR

We next used the purified recombinant proteins to directly determine whether AflR and AflS(MBP) interact with each other *in vitro*. Quantitative information on the strength of the interaction was obtained using microscale thermophoresis (MST) **[20]**. We therefore labeled AflS(MBP) with a 'RED-NHS-ester' fluorophore dye, which reacts covalently with primary amines (lysine amino groups). The labeled AflS(MBP) was then separated from unreacted dye, mixed with non-labelled AflR, and subjected to MST analysis using a Monolith X instrument (NanoTemper Technologies GmbH). A significant increase in the fluorescence was observed upon the addition of AflR before the heating step in MST **(Fig. 2A)**. In contrast, fluorescence intensity did not change when AflR and AflS(MBP) were denatured by heating in the presence of SDS prior to Monolith X measurements (data not shown). Therefore, the interaction between AflR and AflS(MBP) requires correctly folded proteins. A similar experiment performed with 'RED-NHS-ester'-labeled AflR and non-labeled MBP demonstrated no fluorescence increase upon their combination, indicating no protein-protein interaction **(Fig. 2B)**. This result rules out the possibility that AflR and AflS(MBP) interact through the MBP moiety.

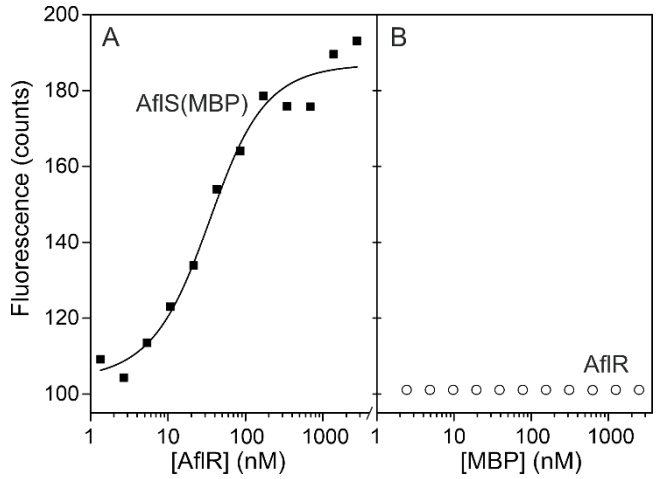

Figure 2. The analysis of AflR·AflS interactions using microscale thermophoresis. (A) AflS(MBP) (20 nM) labeled with the 'RED-NHS-ester' fluorophore was incubated with a dilution series of non-labelled AflR. The line represents the best fit of Equations 1–3. (B) AflR (45 nM) labeled with the 'RED-NHS-ester' fluorophore was incubated with a dilution series of non-labeled MBP. Reported fluorescence values were recorded at 23°C before the activation of sample heating phase of the MST instrument.

The dissociation constant for the AflR·AflS(MBP) complex was obtained by fitting **Equations 1–3**, which take into account decreases in free protein concentrations upon complex formation **[21]**, to the data in **Fig. 2A.** The fitting procedure yielded a $K_{D,R-S}$ value of 24 ± 6 nM (S.E.), indicating a reasonably strong interaction between AflR and AflS (**Fig. S2)**. It is noteworthy that **Equations 1–3**, which consistently modeled the experimental data, assume a simple 1:1 stoichiometry in the AflR·AflS complex.

AflS decreases the DNA-binding affinity of AflR

The DNA binding capabilities of AflR, AflS(MBP), and their mixtures were determined using various models of the *norA* promoter. Previous publications have reported on strong binding of *A. parasiticus* AflR to the *norA* promoter and several other promoters within the AF biosynthesis gene cluster. These studies identified the 5´-TCGN$_5$CGA-3' sequence as the main AflR binding motif on these promoters **[9]**.

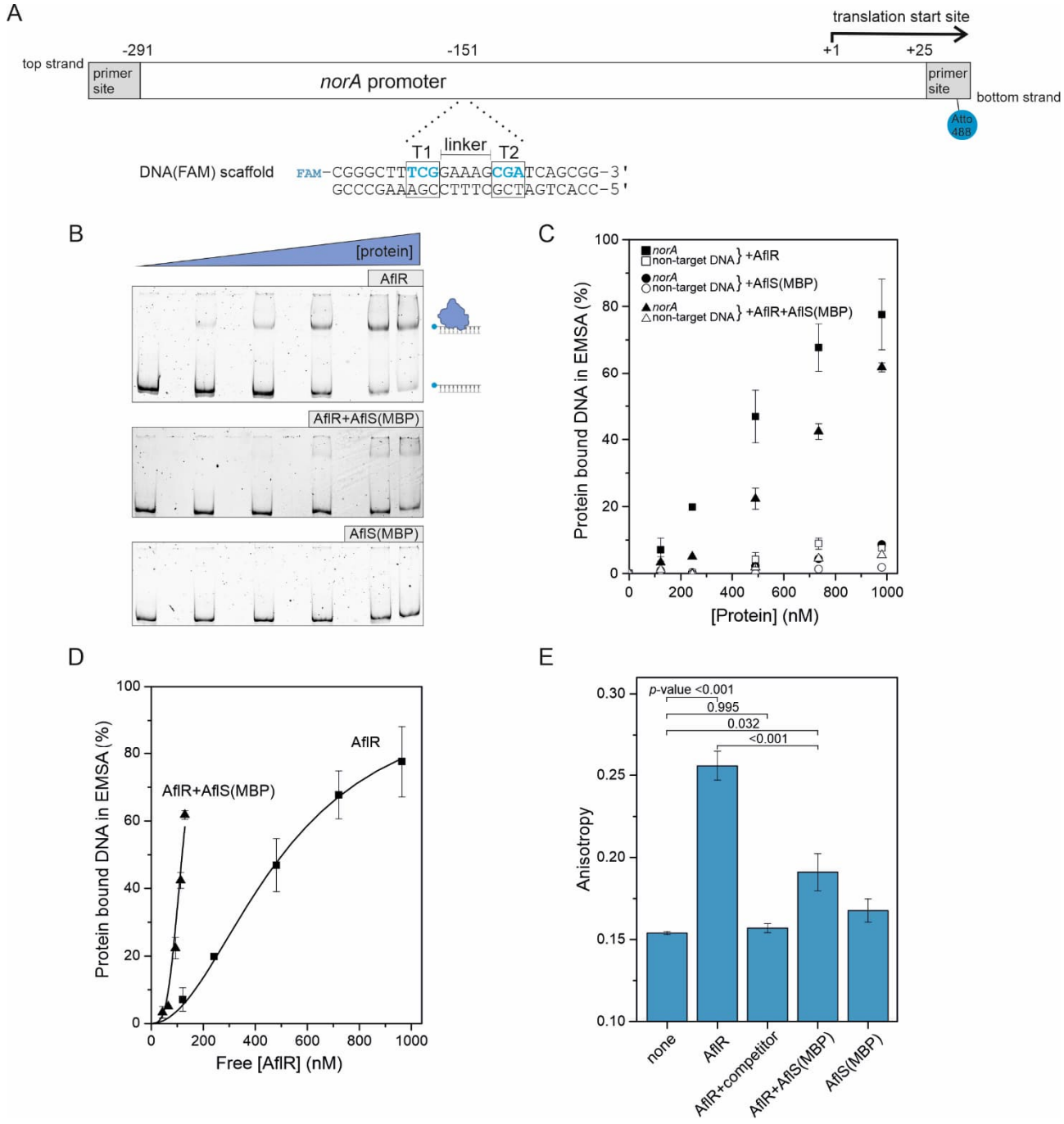

Figure 3. AflS affects the DNA-binding affinity of AflR. (A) A schematic structure of FAM-labelled *norA* promoter DNA used in the EMSA assay. (B) EMSA gels demonstrate the formation of AflR·*norA* complexes at high protein concentrations and the lack of DNA binding by AflS(MBP). The cartoon on the right side indicates the positions of protein-bound and protein-free *norA* DNA on the gel. Atto488-labeled *norA* or non-target DNA (20 nM) was used in all EMSA experiments along with 0–980 nM AflR and/or AflS(MBP). When both AflR and AflS(MBP) were added, the proteins were used in equimolar concentrations. Gel scans from a representative experiment are shown. (C) The percentage of *norA* (filled symbols) or non-target DNA (open symbols) associated with the protein·DNA complex in the EMSA assay. Averages and standard deviations (SD) from three independent experiments are shown. The percentage of protein-bound DNA is shown as a function of total AflR concentration. (D) Same as in panel C, but the percentage of protein-bound DNA is shown as a function of free AflR concentration, obtained by subtracting the concentrations of AflS- and DNA-bound AflR. The trend lines were obtained using Equations 5 or 6 and the best-fit parameter values detailed in the main text. (E) Fluorescence polarization anisotropy of 20 nM DNA(FAM) in the absence of proteins (marked as sample *none*) or 10 min after the addition of 150 nM AflR

(*AflR*), 150 nM AflR and 200 nM unlabeled competitor DNA (*AflR+competitor*), 150 nM AflR and 350 nM AflS(MBP) [*AflR+AflS(MBP)*], or 150 nM AflS(MBP) [*AflS(MBP)*]. The indicated *p*-values for pairwise sample comparisons were obtained using one-way ANOVA with Tukey post hoc test in IBM SPSS Statistics 28.0 software. The null hypothesis, which assumed that fluorescence polarization anisotropy of two samples is the same, was rejected when *p*-value was <0.05.

We first employed EMSA, a technique in which protein binding to DNA reduces DNA migration in the gel. We employed a 369-bp fragment of DNA, which contained the -291/+25 region (where +1 denotes the first base of translation start codon) of *norA* from *A. flavus* NRRL3357, with flanking amplification primer binding sequences. Additionally, we attached an Atto488 fluorophore near the 5' end of the bottom strand for the convenient detection of the DNA by fluorescence scanning **(Fig. 3A)**. The AflR binding motif, specifically 5'-**TCG**GAAAG**CGA**, begins at position -151 of our *norA* promoter construct. As expected, the *norA* promoter exhibited high electrophoretic mobility in the absence of proteins **(Fig. 3B)**. When increasing concentrations of AflR were mixed with the *norA* promoter, a slowly migrating band emerged on the gel, accompanied by a corresponding decrease in the amount of the rapidly migrating DNA component. A similar mobility shift did not occur in experiments using negative control DNA devoid of known AflR-binding motifs **(Fig. 3C**, refer to non-target DNA data**)**. Because such an observation is the hallmark of sequence-specific protein–DNA complex formation, the purified AflR protein is functional and specifically recognizes its target sites on the DNA. In contrast, the addition of AflS(MBP) to the *norA* promoter or negative control DNA did not induce a significant mobility shift, suggesting that this protein does not have binding sites on either DNA.

The addition of AflS(MBP) to 20 nM *norA* promoter together with AflR in a 1:1 ratio, decreased the percentage of slowly migrating DNA (**Figs. 3B and 3C**). Once again, the negative control DNA did not respond to the addition of the AflR and AflS(MBP) mixtures. The effect of AflS(MBP) on AflR binding to DNA could result from a decrease in free AflR concentration due to complex formation with AflS(MBP), provided that this complex does not bind to DNA or, alternatively, binds with lower affinity compared to AflR. To distinguish between these possibilities, we analyzed the binding curves by considering the *free* AflR concentration as an independent variable. It was calculated by subtracting the concentrations of DNA-bound AflR (estimated from band intensities on the gel in **Fig. 3B**) and of the AflR-AflS complex (calculated using the previously determined $K_{D,R-S}$ value of 24 nM) from the total AflR concentration. If the AflR-AflS complex is inert in binding, the binding curves measured in the absence and presence of AflS by varying free AflR concentration should overlap. **Fig. 3D** clearly shows that this is not the case and that the amounts of protein-bound DNA are higher in the presence of AflS at the same free AflR concentrations. The evident implication is that the DNA binds the AflR·AflS complex but with weaker affinity compared to that for AflR binding alone.

Quantitative estimates of the DNA-binding affinities were obtained within the framework of **Scheme 1** by fitting **Equations 5 or 6** to the dependencies shown in **Fig. 3D**. **Scheme 1** assumes that DNA cooperatively binds either two copies of AflR or two copies of the AflR·AflS complex. The models assuming the binding of single copies of either protein resulted in a much poorer fit, whereas assuming the formation of a mixed complex containing one copy each of the proteins did not increase fit quality, based on the sum of the squares of residuals. Moreover, the dissociation constant for the mixed complex binding tended to infinity, ruling out its formation. It is worth noting that the EMSA method is not particularly suitable for quantitative analysis because the measured stability of the protein·DNA complex may be affected by the gel matrix and partial dissociation of DNA·protein complex during the electrophoresis step. Nevertheless, in terms of the apparent dissociation constants deduced from EMSA data, AflS decreased the binding affinity of AflR to the *norA* promoter by twofold: $K_1 = 0.25 \pm 0.03$ μM^2 (AflR binding), $K_2 = 0.54 \pm 0.03$ μM^2 [AflR+AflS(MBP) binding].

To corroborate AflS's role as a modulator of AflR's DNA-binding function using a different method, we employed a short (25 bp) double-stranded DNA oligo scaffold embedded with the AflR-binding motif, identical to that in the *norA* promoter **(Fig. 3A)**. The scaffold also contained a FAM fluorophore, enabling fluorescence polarization anisotropy-based monitoring of protein–DNA interactions directly in solution. We observed that this DNA(FAM) scaffold exhibited low fluorescence anisotropy (~0.15) in the absence of proteins, as expected for a small DNA molecule, which by rapid rotation the DNA molecules relaxed most of the orientation bias in the fluorescently excited state **(Fig. 3E)**. Upon addition of AflR, the anisotropy increased to ~0.25, consistent with the formation of a larger and thus more slowly rotating AflR·DNA(FAM) complex. The formation of the high-anisotropy AflR·DNA complex was blocked when the reaction buffer additionally contained a ten-fold molar excess of unlabeled, but otherwise identical DNA scaffold as a competitor (refer to AflR+competitor sample in **Fig. 3E**). The simultaneous addition of both AflR and AflS(MBP) to DNA(FAM) resulted in a smaller increase in anisotropy (to ~0.20), consistent with the negative effect of AflS(MBP) on the DNA-binding affinity of AflR. In contrast, the addition of AflS(MBP) alone did not significantly change the anisotropy of the DNA(FAM) scaffold, confirming the absence of the DNA-binding function in this protein.

AflR recognizes two specific base triplets and the connecting linker in the DNA

We then investigated the kinetics and sequence determinants of AflR·DNA complex formation and stability. We utilised the same AflR-binding motif-containing short DNA(FAM) scaffold as previously, but recorded fluorescence intensity data using fixed vertical and horizontal positions for the excitation and emission polarizers, respectively, to gather data points more frequently **(Fig. 4A)**. This adjustment to a fixed perpendicular polarizer orientation (⊥) increased the data collection rate of LS55 fluorometer (PerkinElmer) tenfold (to 2 Hz) compared to anisotropy measurements, which involve swapping between horizontal and vertical emission polarizers.

We conducted sequential addition experiments, in which DNA(FAM) solution was first supplemented with AflR and then with non-labeled competitor DNA **(Fig. 4B)**. The fluorescence intensity of DNA(FAM) was relatively high when measured in perpendicular polarizer orientation **(Fig. 4C)**, consistent with the previously measured low anisotropy of this protein-free sample **(Fig. 3E)**. The addition of AflR decreased the intensity by ~15%, indicating the formation of the AflR·DNA(FAM) complex **(Fig. 4B, C)**, which also exhibited higher anisotropy in previous measurements **(Fig. 3E)**. However, the formation of the AflR·DNA(FAM) complex was too fast to be kinetically resolved, primarily because of a ~20-s dead time caused by protein addition and mixing steps. Subsequent addition of wild-type (WT) competitor DNA scaffold, which is identical to DNA(FAM) but lacks a fluorophore, triggered a slow increase in fluorescence intensity, consistent with the dissociation of the AflR·DNA(FAM) complex and subsequent sequestration of AflR by the competitor DNA (**Fig. 4C**, WT trace). The dissociation kinetics was biphasic with the lifetime parameters (t) of 51 ± 7 and 575 ± 16 s, respectively. The corresponding dissociation rate constants ($k = 1/t$) are 0.020 ± 0.003 s^{-1} and 0.0017 ± 0.0001 s^{-1}. All fit parameters are listed in **Fig. S3A**. Based on the sum of two amplitudes (A_1 and A_2) fluorescence intensity of DNA(FAM) recovered to the initial protein-free level when WT DNA competitor was used. This behavior was expected due to the large excess (50-fold) of the unlabeled DNA competitor over DNA(FAM).

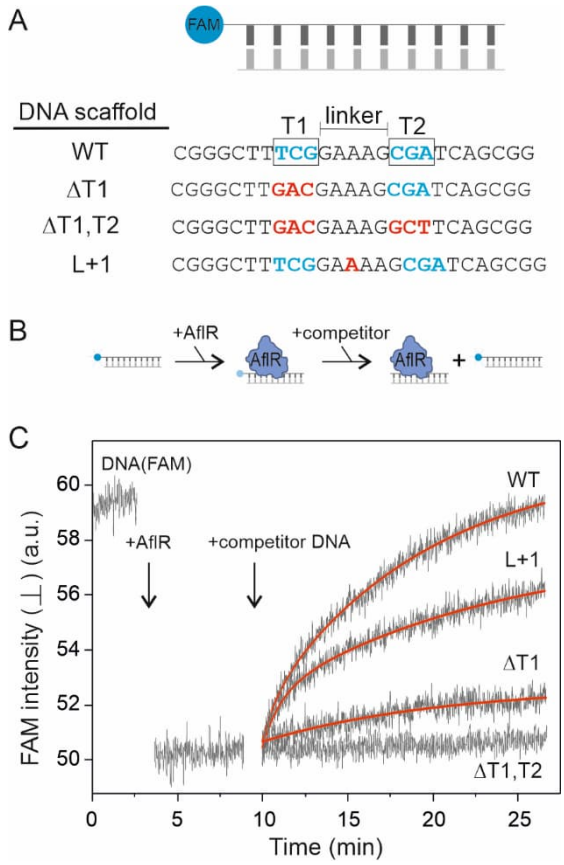

Figure 4. Kinetics and sequence determinants of AflR·DNA complex formation and stability. (A) The structures of the DNA scaffolds used to monitor the formation and dissociation of AflR·DNA complex. Non-template (top) and template (bottom) DNA strands are shown in dark and light grey, respectively. The blue sphere represents the FAM fluorophore attached to the 5' end of the non-template DNA strand. The sequences of the non-template strands of wild-type and mutated DNA scaffolds are shown. The competitor scaffolds were not labeled with FAM. The triplet sequence motifs T1 and T2 (shown in blue) and the linker (L) in the AflR-binding region in the wild-type DNA scaffold are highlighted. DNA mutations are indicated in red font in the competitor scaffolds with one (ΔT1) or both (ΔT1,ΔT2) base triplets substituted, or the linker extended by 1 bp (L+1). (B) The order of additions in the kinetic measurement. The initial fluorescence of 20 nM DNA(FAM) scaffold was measured before adding 330 nM AflR to the fluorometer cuvette. The formed AflR·DNA(FAM) complexes were disrupted by the further addition of 1000 nM unlabeled competitor DNA scaffold. (C) The kinetics of fluorescence changes. The fluorescence decreased after AflR addition, indicating AflR·DNA(FAM) complex formation. The addition of WT, L+1, or ΔT1 competitor DNA caused full or partial gradual disruption of the AflR·DNA(FAM) complexes accompanied by fluorescence increase. The lifetime of the AflR·DNA(FAM) complex was estimated by fitting 1- or 2-phase exponential decay equations to the dissociation part (after ~10 min) of the reaction progress curves. The parameter values derived from the red fit curves are shown in Figure S3A. Fluorescence intensity was recorded using the fixed perpendicular orientation (⊥) for the excitation and emission polarizers, respectively, and was corrected for the dilution caused by AflR and competitor additions. Experiments were performed at 23°C and repeated three times. Representative traces are shown.

We next employed the assay to evaluate the binding efficiency of mutant competitor DNAs, in which specific functional parts of the AflR-binding sequence motif, previously recognized **[8,9]**, were modified. Specifically, we modified the two palindromic base triplets (T1 and T2 in **Fig. 4A**) and the linker (L) connecting them. Fluorescence measurements indicated that the DNA completely lost its competitor potency when both base triplets were substituted (ΔT1, T2 trace in **Fig. 4C**). When only one triplet was substituted, the DNA functioned as a competitor but with significantly decreased potency; the decrease in the binding affinity was inferred from the fact that fluorescence

recovered by only 24% after the addition of ΔT1 competitor (**Fig. 4C**, see also amplitude parameter A_1 in **Fig. S3A**). The extension of the linker by 1 bp was less damaging to the binding efficiency, as this competitor DNA recovered 75% of the initial fluorescence intensity (L+1 trace in **Fig. 4C**, see also amplitude parameters A_1 and A_2 in **Fig. S3A**).

AflR binding to DNA labelled with a Cy3 fluorophore

To exclude potential dye artefacts and further improve spatial and temporal resolution of the binding assay, we replaced FAM with Cy3 in the DNA scaffold embedding the AflR-binding motif [referred to as DNA(Cy3)]. The Cy3 fluorophore was chosen because its intensity often substantially increases when a protein binds to a nearby site on the DNA **[22]**. This increase in Cy3 fluorescence is due to its cis/trans photoisomerisation, a phenomenon typically referred to as protein-induced fluorescence enhancement (PIFE). Indeed, the addition of AflR to the DNA(Cy3) sample resulted in a rapid increase in the fluorescence intensity by approximately 30%. This PIFE effect indicates that AflR binds, as expected based on the orientation of AflR binding motif, near Cy3 **(Fig. S3B)**. The effects of non-labelled competitor DNA scaffolds on the AflR·DNA(Cy3) complex paralleled those observed using the DNA(FAM) scaffold (as described above). Specifically, the addition of WT competitor triggered a slow biphasic decrease in fluorescence intensity, consistent with the dissociation of all AflR·DNA(Cy3) complexes. The scaffold with a 1-bp extended linker (L+1) acted as a reasonably effective competitor, whereas the elimination of one of the two triplet motifs in ΔT1 scaffold led to a weaker competitor efficiency.

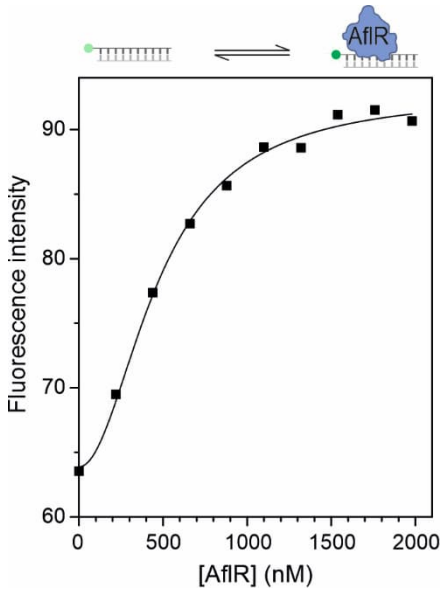

Figure 5. Equilibrium binding of AflR to short target DNA. The DNA(Cy3) scaffold (20 nM) was titrated with increasing concentration of AflR at 23°C. The curve was obtained using the equation and parameter values shown in Fig. S3C.

To probe the AflR's affinity to DNA(Cy3) in a different experimental setup, we determined the response of DNA(Cy3) fluorescence to AflR concentration at equilibrium using a conventional spectrofluorometer. The obtained data revealed that the overall PIFE effect of DNA(Cy3) levels off, i.e., both binding sites of AflR become saturated at micromolar AflR concentrations **(Fig. 5)**. The binding curve could be described by the cooperativity model similar to that used to describe AflR binding to *norA* in the EMSA assay shown in **Fig. 3D**. Once again, because of high cooperativity, separate binding constants for two sites could not be estimated with a reasonable precision. However, their product (0.23 ± 0.02 μM^2; **Fig. S3C**) was in an excellent agreement with that obtained from **Fig. 3D** for AflR binding to long *norA* promoter (0.25 ± 0.03 μM^2).

Rapid kinetics supports sequential binding of two AflR molecules to the recognition site in DNA

Combining AflR with the DNA(Cy3) scaffold resulted in a rapid increase in the fluorescence intensity **(Fig. S3B)**, unresolvable in the manual mixing experiments. We therefore employed a stopped-flow instrument to automate the mixing of AflR from one syringe with DNA(Cy3) from the other syringe, thereby reducing the mixing dead time to 2 ms (**Fig. 6A, B**). We performed this experiment at several AflR concentrations (20–330 nM), keeping the DNA concentration fixed at 20 nM. The stopped-flow data showed an increase in Cy3 fluorescence intensity shortly (~0.1 s) after mixing the DNA with AflR, reaching maximum in about 30 s (**Fig. 6B** and **Fig. S4A-D**). Interestingly, increasing the AflR concentration resulted in a larger increase in fluorescence intensity, but not in a faster rate of fluorescence change.

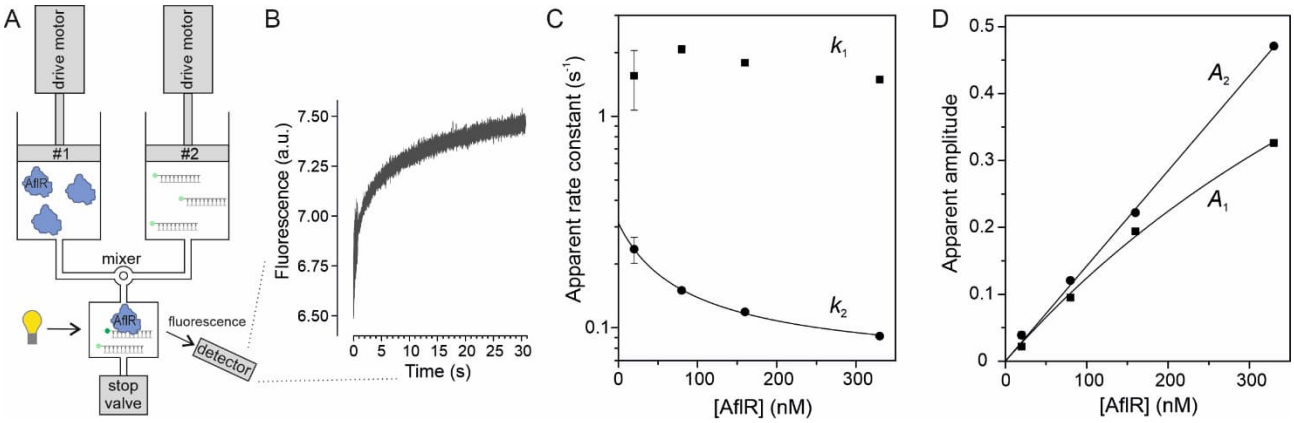

Figure 6. Stopped-flow kinetic analysis of AflR·DNA complex formation. (A) Experimental setup of the stopped-flow instrument. (B) An example trace demonstrating the increase in fluorescence intensity of 20 nM DNA(Cy3) after mixing with 330 nM AflR at 23°C. Apparent binding rate constants k_1^{app} and k_2^{app} (C) and signal amplitudes A_1^{app} and A_2^{app} (D) were obtained by fitting a 2-phase exponential equation to the measured fluorescence intensity traces as shown in Fig. S4. The theoretical curves for A_1 is derived from the fit with Equation 7. The trend of A_2 is derived from a linear fit and is shown for visualization purposes.

As the first step towards extracting quantitative information, we evaluated which exponential equation most robustly describes the stopped-flow traces **(Fig. S4E)**. To this end, we assessed the quality of the fits for different models visually **(Fig. S4A-D)** and based on the sum of the squares of residuals (RSS) **(Fig. S4F)**. The simplest, 1-phase exponential model exhibited systematic deviation of the best-fit curves from the data and large RSS values, especially at high [AflR]. The exponential equations assuming 2 or 3 phases demonstrated very similar RSS values (less than 5.1% difference). We conclude that the 2-phase exponential model is the simplest one adequately describing the data.

The 2-phase nature of the stopped-flow data implies that two molecular processes contribute to the fluorescence enhancement. Clues to the nature of these processes were provided by the analysis of the output parameters of the fit (**Fig. S4G**), which include two rate constants (k_1 and k_2) and two amplitude factors (A_1 and A_2). The k_1^{app} value appeared to be constant over the entire range of [AflR], whereas k_2^{app} decreased with increasing [AflR] (**Fig. 6C**; for a linearly scaled ordinate, see **Fig. S4H**). Importantly, neither of the rate constants increased with [AflR], which excludes the possibility that they refer to the AflR binding step. Instead, the stepwise fluorescence enhancement probably results from conformational changes in the preformed AflR·DNA complex. The relative amplitudes of the two signals were similar at any [AflR], whereas the absolute values increased almost linearly with [AflR] (**Fig. 6D**), consistent with the low degree of DNA saturation with AflR at the concentrations used in the stopped-flow experiments (**Fig. 5**). The binding affinity of the DNA(Cy3) scaffold for the first AflR molecule could be roughly estimated from the AflR

concentration dependence of A_1^{app} (**Fig. 6D**) using **Eq. 7**. The obtained value (820 ± 250 nM) and other parameters are shown in **Fig. S4I**. The high sample consumption of the stopped-flow instrument prohibited us from probing the effects of higher AflR concentrations on the kinetic parameters of DNA(Cy3) binding, which potentially could have decreased the uncertainty in the estimate.

The simplest kinetic scheme explaining the stopped-flow data (**Scheme 1**) presumes that the initial binding of two AflR molecules to DNA, yielding the DNA·AflR and DNA·AflR$_2$ complexes, reaches equilibrium within the dead-time of the instrument. Then, both complexes isomerize with the rate constants k_1 and k_2, respectively, causing a change in Cy3 fluorescence. This simple scheme cannot, however, explain the decrease in k_2 at high AflR concentrations, because isomerization is a monomolecular process, which should be independent of medium AflR concentration. The observed decrease in k_2 suggests the formation of a stoichiometrically distinct complex, and one possibility, to be tested in future work, is AflR oligomerization at high concentrations. One can further speculate that DNA can bind the oligomerized AflR, but the isomerization reaction proceeds slower if one recognition site contains AflR oligomer. AflR binding to a third site on DNA with a K_D of approximately 40 nM (as derived from **Fig. 6C**) is a less likely alternative explanation of the variation in the k_2 value.

Discussion

The AF biosynthesis gene cluster includes two pathway-specific regulators: AflR, a sequence-specific DNA-binding protein that activates the transcription of most AF cluster genes, and AflS **[2,3,5,6,8,9,11]**. While AflR is essential for AF biosynthesis, AflS, while not deemed critical, seems to solely enhance AF accumulation in *Aspergillus* cultures through mechanisms that remain incompletely understood **[11,14,15]**. In this study, we aimed to provide further clarity on the molecular mechanisms of AflR and AflS, specifically focusing on the question how AflR recognizes its target sites on the DNA and how AflS modulates this process. Deeper insight into the regulatory mechanisms of AF biosynthesis may help develop strategies to disrupt toxin production, engineer resistant crops, and improve detection methods, ultimately leading to better food safety.

To study the function and interplay of AflR and AflS in detail at the molecular level, we first developed the protocols to obtain milligram quantities of highly purified, full-length proteins. During the process we found both proteins to be prone to aggregation but managed to remedy the problem by expressing the recombinant AflR in a specific *E. coli* strain (BL21[DE3]) at low temperature (16^{o}C) or including N-terminal MBP-tag in AflS. To the best of our knowledge, our protocol to prepare recombinant AflS in sufficient quantities for biochemical and structural studies is the first published. Our AflR protocol simplifies the preparation of full-length protein and may provide a more homogenous sample by avoiding the refolding step, which was previously used to recover *A. nidulans* AflR from *E. coli* inclusion bodies **[8]**.

Earlier, evidence for complex formation between AflR and AflS of *A. parasiticus* was obtained using a two-hybrid assay, wherein genes of both proteins were co-expressed in *Saccharomyces cerevisiae* **[16,17]**. Considering that their interaction in the cell could be mediated or modulated by other yeast proteins, we used the purified AflR and AflS to determine whether they directly interact *in vitro*. Indeed, our biophysical data confirmed that AflR and AflS form a complex in the absence of other proteins and provided the first quantitative estimate for the stability of this complex ($K_{D,R–S}$ 24 ± 6 nM) (**Fig. 2A**). Our analysis further indicated a simple 1:1 protein stoichiometry in the AflR·AflS complex. Previously, based on indirect evidence derived from the comparison of *aflR* and *aflS* transcript levels in the conditions permissive and non-permissive for AF production, respectively, it was suggested that four AflS protein molecules bind to a single AflR protein molecule to form an activated transcription regulation complex **[23]**. The binding curve in **Fig. 2A** is, however, inconsistent with such stoichiometry.

We employed EMSA, anisotropy and PIFE assays to provide the first quantitative analysis on how AflR and AflS interact with the DNA. Sequence annotation tools predict AflS to contain a structure region similar to a winged helix DNA-binding domain (e.g., see entry O42716 in uniprot.org). In contrast to this prediction, we did not observe *in vitro* any binding of AflS to *norA* promoter or the negative control DNA. A previous ChIP-based study also provided no evidence for AflS binding to four tested AF gene cluster promoters (*aflJ*, *fasB*, *pksA* or *ver1*) *in vivo* using ChIP assay **[17].** Collectively these results suggest that either AflS is not a DNA binding protein or, less likely, AflS has such a narrow DNA binding specificity that it so far avoided detection. In contrast, the DNA binding signal of AflR was clear in our assays, and the concentration dependence indicated that two AflR molecules bind per one DNA target site (**Fig. 3D** and **Fig. 5**). Time-resolved analysis of the AflR·DNA complex formation, using stopped-flow fluorescence recordings with the dead-time of 2 ms, provided further support for the notion that two AflR monomers bind successively to the target DNA (**Fig. 6**). Furthermore, the independence of the apparent rate of fluorescence enhancement on the AflR concentration indicated that initial AflR·DNA complexes form fast, probably near diffusion controlled limit, and then undergo slower conformational changes to the final structure. The slow release of AflR from the target DNA **(Fig. 4C, S3B)** indicates strong kinetic stability of the final AflR·DNA complex. This finding is consistent with the ChIP-based detection of AflR on the chromatin DNA in the cell **[12,17]**.

The formation of AflR·DNA complex was nearly saturated at about 1 μM AflR; however, the binding affinity of AflR·AflS complex to *norA* promoter model DNA, in the terms of dissociation constants (0.54 vs. 0.25 μM^2), was twofold less than for AflR alone (**Fig. 3**). The negative modulation of the DNA binding affinity of AflR by AflS was a surprising finding provided that the AF biosynthesis co-activator function of AflS is firmly documented **[11,14,15]**. One purely speculative explanation is that moderate down-tuning of the AflR's DNA-binding affinity would preferentially release AflR from low-affinity nonspecific binding sites on the chromatin DNA, thereby targeting more AflR·AflS complexes to the high-affinity binding sites in the promoters of the AF gene cluster. It can be further speculated that AflS may serve to facilitate AflR in recruiting additional regulatory transcription factors and/or core components of RNA polymerase II apparatus to promoters, thus increasing the expression of AF biosynthetic genes. Further studies aiming to correlate the protein composition (by mass spectrometry) and transcriptional activity (by RT-PCR or RNA-seq) of specific AF pathway promoters are required to test the above hypotheses. Our data predicts, based on the relatively high strength of AflR·AflS complex ($K_{D,R-S}$ 24 ± 6 nM), that AflR is able to recruit AflS to the AF gene cluster promoters via direct protein–protein interaction, thereby providing a platform for the recruitment of additional proteins.

The effects we observed for the sequence perturbations in the AflR binding site in the DNA are overall consistent with the previous model **[8,9]**, in which AflR interacts with two specific base triplets separated by a compatible distance (linker or spacer). The ideal linker length appears to be 5 bp based on our and previous results **[8,9]**, however, one specific inference from our data was the retention of reasonable competitor function of the DNA with the 6-bp linker, indicating that AflR can accommodate at least small variations in the linker structure **(Fig. 4C)**. Moreover, because we employed full-length AflR and the previous studies employed partial AflR proteins lacking about 10% (*A. nidulans* AflR) **[8]** or 50% (*A. parasiticus* AflR) **[9]** of native C-terminal amino acid residues (which are part of the transcription activation domain of AflR), it is now possible to conclude that the C-terminal half of the protein does not contribute significantly to the DNA binding specificity of AflR. The sequence identities between *A. nidulans* and *A. parasiticus* AflR and AflR from *A. flavus* explored in this study are 33% and 98%, respectively. The similarity of the data from different studies indicates strong interspecies conservation of the DNA-binding specificity of AflR.

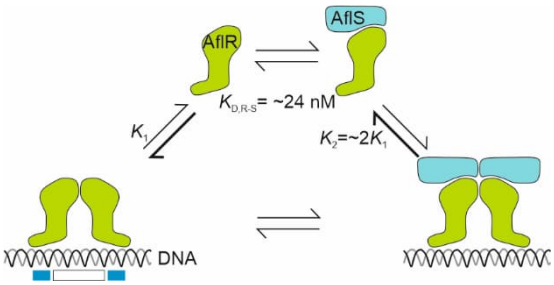

Figure 7. Model illustrating the interaction of AflR with AflS and their binding to the target site on DNA. AflR forms a protein complex with AflS, both in DNA-free and DNA-bound states, with a dissociation constant of approximately 24 nM. Cooperative binding of two AflR molecules, either individually or in complex with AflS, occurs at the target DNA site. The strength and specificity of the binding site primarily depend on the sequence of two 3-bp motifs (highlighted by blue rectangles) and the length of the linker (depicted as a white rectangle) connecting them. Notably, AflS reduces the DNA binding affinity of AflR twofold ($K_2 > K_1$).

To summarize our findings, we propose a working model of AflR and AlfS functioning as aflatoxin gene cluster regulators (**Fig. 7**). The first significant element of the model is the protein-protein interaction between AflR and AflS both in the DNA-free and DNA-bound state. AflS reduces the DNA binding affinity of AflR twofold, but on the other side, AflR may recruit AflS to the promoters of AF gene cluster, constituting a platform for the recruitment of transcription apparatus and other regulatory proteins. Two AflR molecules or AflR·AflS complexes bind cooperatively to the DNA target site and undergo a rate-limiting conformational change to the final structure. The affinity of the binding site primarily depends on the DNA sequences of two 3-bp motifs and the length of the linker connecting them.

Materials and methods

Genes, oligonucleotides and reagents

HPLC-purified non-labelled and PAGE-purified FAM- or Cy3-labelled oligonucleotides for DNA binding assays were purchased from Merck. To prepare double-stranded DNA scaffolds for binding assays, two complementary single strands were mixed at 10 µM each in MQ water, heated to 70ºC for 5 min and gradually cooled (~5ºC/min) to 21ºC in a thermo shaker (Brant-Bio). All PCRs were performed with the Phusion™ High-Fidelity DNA Polymerase Kit (Thermo Fisher Scientific), and the primers synthesized by Eurofins Genomics. Restriction enzymes, DNA size markers, T4 DNA ligase, and Gibson assembly master mix were purchased from New England Biolabs (NEB). A nickel–nitrilotriacetic acid (Ni^{2+}-NTA) superflow metal-affinity chromatography matrix, specifically PureCube 100, was obtained from Cube Biotech. Tris base, β-mercaptoethanol (β-ME), phenylmethylsulfonyl fluoride (PMSF), lysozyme, maltose, TEMED, and agarose were from Merck (Sigma-Aldrich). EDTA was acquired from VWR chemicals, $ZnSO_4 \cdot 7H_2O$ was from Scharlau, and tryptone and yeast extract were from Neogen. The remaining chemicals and kits were purchased from Thermo Fisher Scientific.

Construction of expression plasmids

The protein sequences of *A. flavus* AflR (34 sequences) and AflS (10 sequences) were collected from GenBank. The sequences were aligned and analyzed using Mega 7 **[24]**. AflR sequences contained 437–444 amino acid residues **[25]** and exhibited a mean identity of 97.9% (indels discarded from analysis). AflS sequences contained 376–439 amino acid residues and showed a mean identity of 99% (indels discarded). The consensus AflR and AflS sequences were calculated using EMBOSS Cons software (https://www.ebi.ac.uk/Tools/msa/emboss_cons/) **[26]**.

The derived AflR consensus sequence consisted of 444 amino acid residues and was identical to GenBank® sequence AAW32195.1 **[27]**. The derived AflS consensus sequence comprised 438 amino acid residues and was identical to RMZ43274.1 **[28]**. To facilitate protein purification, we added a histidine tag and a TEV protease cleavage site to the N-terminus of recombinant proteins. The protein coding DNA sequences were optimized for *E. coli* and ordered as either as synthetic protein expression plasmids (AflR and AflS) or gene fragments (MBP and *norA* promoter) from Twist Bioscience. The vector backbone for the expression vectors was pET-21(+), in which the gene-of-interest was placed between NcoI and XhoI restriction sites. The resulting expression plasmids, pAM068 and pAM069, were used to produce AflR and AflS, respectively.

To increase AflS solubility, we added MBP to the N-terminal side of AflS **[29]**. MBP was ligated, using T4 DNA ligase (Thermo Fisher Scientific), to NcoI and NdeI restriction sites in pAM069 to obtain expression construct pAM073 (a TEV protease cut site was included between MBP and AflS). To estimate the effect of the MBP moiety on AflS behavior in the chimeric MBP-AflS protein, MBP was separately expressed from pAM074 (the MBP gene was placed between NcoI and XhoI, constructed from pAM073). All expression plasmids were verified by Sanger sequencing the region encoding transcription control elements and protein-of-interest (Eurofins Genomics).

Protein expression and purification

For protein production, the pAM068 plasmid (to produce AflR), pAM073 [AflS(MBP)], or pAM074 (MBP; the production and purification of MBP are detailed in the Supplementary Material) was transformed into *E. coli* strain BL21 (DE3) and cultured in Luria-Bertani (LB) agar at 37°C. A single colony from the plated transformants was inoculated into 100 mL of LB medium supplemented with 100 µL of 100 mg/mL ampicillin and grown overnight at 37°C. One liter of LB medium (10 g tryptone, 5 g yeast extract, and 5 g sodium chloride dissolved in 1 L Milli-Q water) was supplemented with 1 mL of 100 mg/mL ampicillin and 20 mL of the overnight culture, and the mixture was grown at 37°C in a shaking incubator in four 2 L Erlenmayer flasks (Multitron, Infors HT) at 250 rpm. When the A_{600} reached 0.5, the culture was transferred to 4°C for 40 min, and protein expression was induced overnight by adding 0.5 mM IPTG while maintaining the temperature at 16°C with shaking at 170 rpm. The cells were harvested by centrifugation at 6000 g, 4°C for 15 min and stored at -80°C until protein purification.

For AflR purification, the cells were resuspended in 45 mL of lysis buffer R (50 mM Tris-HCl, pH 6.9, 0.5 M $(NH_4)_2SO_4$, and 5% glycerol) supplemented with 1 mM β-mercaptoethanol (β-ME) and 0.1 mM phenylmethylsulfonyl fluoride (PMSF). Subsequently, 1 mg/mL lysozyme was added, and the suspension was incubated on ice for 30 min. The cells were then disrupted by sonication (5 times of 30 s with 5 min incubations on ice in between). The lysate was cleared by centrifugation at 39,000 g at 4°C for 30 min. The supernatant was supplemented with 10 mM imidazole (stock pre-adjusted to pH 7.0 with HCl) and loaded onto a PD10 gravity column (Cytiva) containing about 1 mL bed of Ni-NTA agarose (PureCube 100, Cube Biotech), which had been pre-equilibrated with the lysis buffer R. The column was washed with 10 mM imidazole in lysis buffer for removing loosely bound proteins. AflR was eluted using 0.3 M imidazole in the lysis buffer R. The eluted protein was concentrated to a final volume of 3 mL using Amicon® Ultra-4 centrifugal filter (Merck Millipore,). The concentrated protein was then injected into a gel filtration column (HiLoad 16/600 or 26/600 Superdex 200 prep grade; GE Healthcare) that had been pre-equilibrated with a gel filtration buffer (50 mM Tris-HCl, pH 6.9, 5% glycerol, 0.5 mM EDTA, and 0.5 M $(NH_4)_2SO_4$). AflR was eluted with the gel filtration buffer at a flow rate of 0.1 mL/min using Äkta Purifier system (GE Healthcare). AlfR-containing fractions were concentrated to about 0.2 mL using Amicon® Ultra-4 centrifugal filter, aliquoted and stored at -80°C.

For the purification of AflS(MBP), the cell pellet was resuspended in lysis buffer S (50 mM Tris-HCl, pH 7.9, 0.5 M KCl, 5% glycerol, 1 mM β-ME, 20 µM $ZnSO_4$) supplemented with 0.1

mM PMSF. Then 1 mg/ml lysozyme was added and mixture was incubated on ice for 30 min. The cells were then disrupted by sonication (5 times of 30 s, with 5 min of incubations on ice in between). The lysate was cleared by centrifugation at 37,000 g for 30 min at 4°C. Proteins in the supernatant were precipitated by slowly adding solid ammonium sulfate to final concentration 300 g/L followed by centrifugation at 37,000 g for 30 min at 4°C. The resulting pellets were resuspended to lysis buffer S supplemented with 10 mM imidazole and 0.1 mM PMSF, and loaded onto a PD10 gravity column (Cytiva) containing about 1 mL bed of Ni-NTA agarose (PureCube 100, Cube Biotech), which had been pre-equilibrated with the lysis buffer S. The column was washed with 10 mM imidazole in lysis buffer S to remove loosely bound proteins. AflS(MBP) was eluted using 0.3 M imidazole in the lysis buffer S followed by the dilution of the KCl concentration in the eluate to 150 mM using buffer A (50 mM Tris-HCl, pH 7.9, 5% glycerol, 1 mM β-ME, and 20 µM $ZnSO_4$). The sample was then loaded onto a RESOURCE Q column (6 mL column, GE Healthcare), which had been pre-equilibrated with 10% buffer B (buffer A supplemented with 1 M KCl), using a syringe pump unit. AflS(MBP) was eluted from the column using a gradient of 10–100% buffer B at flow rate 1 mL/min; AflS(MBP) eluted at about 300 mM KCl using ÄktaPrime Plus system (GE Healthcare). The fractions containing AflS(MBP) were combined and further purified by loading the sample with a syringe pump (1 mL/min flow rate) onto a dextrin sepharose column (MBPTrap HP column, 1 mL, GE Healthcare), which had been pre-equilibrated with lysis buffer S. The column was washed with 5 mL of lysis buffer S followed by the elution of AflS(MBP) with 5 mL of 20 mM maltose in lysis buffer S. AlfS(MBP) was concentrated to a final volume of about 0.15 mL using Amicon® Ultra-4 centrifugal filter, aliquoted and stored at -80°C.

MBP protein was purified for use as a negative control in AflS(MBP) experiments. The detailed purification protocol of MBP can be found in the Supplementary Materials. For purity analysis, trichloroacetic acid-precipitated proteins **[30]** were separated on NuPAGE Bis-Tris gels (Thermo Fisher Scientific) and visualized either using Coomassie staining or Western analysis with an anti-His tag antibody (6X His Tag Antibody Dylight™ 800 Conjugated, #200-345-382, Rockland), as previously described by **[31]**. PageRuler™ Plus prestained protein ladder (Thermo Fisher Scientific), PageRuler™ prestained protein ladder (Thermo Fisher Scientific) or 6xHis Protein Ladder (cat. no. 34705, Qiagen) were employed as the molecular mass markers. The gel was scanned using an LI-COR Odyssey Infrared Imager. Protein concentrations were estimated based on absorbance at 280 nm using a NanoDrop 2000 spectrophotometer (Thermo Fisher Scientific).

Molecular interaction between AflR and AflS

The interaction between AflR and AflS was monitored using MicroScale Thermophoresis technique (MST). To this end, AflS(MBP) was covalently labeled with lysine residues using the protein labeling kit RED-NHS 2nd generation (NanoTemper Technologies). Unreacted dye was removed using the B-column of the kit. A serial dilution of AflR was prepared, with 10 µL in each vial, and 10 µL of the labeled AflS(MBP) in the binding buffer (20 mM Tris-HCl, pH 7.9, 30 mM KCl, 5% glycerol, and 10 µM $ZnSO_4$) was added to each vial. The samples were mixed by pipetting, incubated for 30 min in the dark at 23°C, centrifuged for 5 min at 12,000 g, and loaded into glass capillaries **[32]**. The MST of the samples **[33]** was performed using Monolith X (MM-078, NanoTemper Technologies). Because the largest change upon the formation of the AflS·AflR complex was observed in the fluorescence before the heating phase of MST, this data was used for quantitative analysis. The dissociation constant of the AflS·AflR complex ($K_{D,S-R}$) was estimated by fitting **Equations 1–3** to the measured initial fluorescence values (F_{total}, the *y* axis of **Fig. 2**). The remaining parameters in **Equations 1–3** are the fluorescence intensity of free AflS (F_S), and the fluorescence intensity of AflS·AflR complex (F_{SR}). $[R_{total}]$ is the total concentration of unlabeled AflR (the *x* axis of **Fig. 2**), $[S_{total}]$ is the total concentration of labeled AflS, $[SR]_{fraction}$ is the fraction

of AflS bound to AflR, and $[S]_{fraction}$ is the fraction of AflS free in solution. All data fitting routines were performed using Origin 2016 (OriginLab Corporation).

$$[SR]_{\text{fraction}} = \frac{([S_{\text{total}}]+[R_{\text{total}}]+K_{D,S-R})-\sqrt{([S_{\text{total}}]+[R_{\text{total}}]+K_{D,S-R})^2-4\times[S_{\text{total}}]\times[R_{\text{total}}]}}{2\times[S_{\text{total}}]} \quad \text{Eq. 1}$$

$$[S]_{\text{fraction}} = 1 - [SR]_{\text{fraction}} \quad \text{Eq. 2}$$

$$F_{\text{total}} = [S]_{\text{fraction}} \times F_S + [SR]_{\text{fraction}} \times F_{SR} \quad \text{Eq. 3}$$

Native acrylamide gel electrophoresis for mobility shift assay (EMSA)

EMSA was performed to characterize AflR and AflS binding to *norA* promoter DNA or negative control DNA devoid of known AflR binding motifs. Both DNA fragments were amplified using PCR and purified with GeneJET gel extraction kit (Thermo Fisher Scientific). The *norA* DNA fragment (length 369-bp) contained promoter region from position -291 to +25 relative to the translation start site at +1, upstream/downstream linkers with primer binding sites, and Atto488 fluorophore in the bottom strand at the 6th position from the downstream edge of the fragment (**Fig. 3A; Fig. S5A**). The negative control DNA (length 507-bp) had the same primer binding and Atto488 attachment sites (**Fig. S5B**). For the binding reactions, a 10 µL reaction mixture was prepared with 20 nM of DNA in binding buffer, with varying concentrations of AflR, AflS(MBP), or their combination. The mixtures were incubated at 23ºC for 30 min before separating the free and protein-bound DNA using native polyacrylamide gel electrophoresis (PAGE). PAGE gel (5%) was prepared in 0.5X TBE buffer (45 mM Tris, 45 mM boric acid, 1 mM EDTA; Thermo Fisher Scientific) and run at 100 V for 90 min. The gel was then rinsed with MQ water and scanned using Azure Sapphire Biomolecular Imager (Azure Biosystems) in the 488 nm channel. The percentages of protein-bound and free DNA were determined from gel band intensities using ImageJ software (https://imagej.nih.gov/ij/). All experiments were done at 23°C at least in duplicate, unless otherwise noted.

The EMSA data were analyzed in terms of **Scheme 1**, which assumes simultaneous binding of two AflR molecules alone or in complex with AflS (ultimate positive cooperativity). The dissociation constants of the DNA·protein complexes, K_1 and K_2, whose dimension is µM^2, were derived by fitting **Equation 4**, where Y represents the percentage of protein-bound DNA, [R] and [R·S] are the concentrations of AflR and the AflR·AflS complex, respectively.

Scheme 1. AflR and AflS binding to DNA. D, R, and S are DNA, AflR, and AflS, respectively, R·S is the complex of AflR with AflS, K_1 and K_2 are the dissociation constants.

$$DR_2 \overset{K_1}{\leftrightarrows} D \overset{K_2}{\leftrightarrows} D(R\cdot S)_2$$

$$Y = 100\,(1 + K_1[R\cdot S]^2/K_2[R]^2)/(1 + K_1[R\cdot S]^2/K_2[R]^2 + K_1/[R]^2) \quad \text{Eq. 4}$$

If AflR binding is measured in the absence of AflS, **Equation 4** reduces to **Equation 5**:

$$Y = 100/(1 + K_1/[R]^2) \quad \text{Eq. 5}$$

If AflR and AflS are present in equimolar amounts, **Equation 4** reduces to **Equation 6**, where $K_{D,S-R}$ = 24 nM is the dissociation constant of the AflR·AflS complex determined in the present work.

$$Y = 100\,(1 + K_1[R]^2/K_{D,R-S}K_2)/(1 + K_1[R]^2/K_{D,R-S}K_2 + K_1/[R]^2) \quad \text{Eq. 6}$$

Fluorescence anisotropy- and intensity based DNA-binding assays

Fluorescence anisotropy and intensity were measured with a LS-55 fluorescence spectrofluorometer (Perkin Elmer) equipped with a quartz cuvette (16.160-F/Q/10, Starna Scientific Ltd, min. sample vol. 160 µl). The excitation and emission wavelengths were set to 480 nm (excitation) and 520 nm (emission) for the DNA(FAM) samples, and changed to 550 and 565 nm for the DNA(Cy3) samples. The excitation and emission slits were kept at 10 nm in all measurements. For anisotropy measurement the excitation light was polarized with a filter to vertical plane whereas the emission light was recorded successively through a vertical and a horizontal polarizer. To achieve increased temporal resolution in **Fig. 4C**, the fluorescence intensity of DNA(FAM) was measured using the excitation and emission polarizers in fixed vertical and horizontal positions, respectively. The fluorescence intensity of DNA(Cy3) was recorded without polarizers.

A 200-µL reaction mixture containing 20 nM labelled DNA in binding buffer was titrated with AflR or AflS(MBP), or their combination with 5-min incubations in the dark after each protein addition. In competition experiments, the fluorescence intensity of 20 nM DNA(Cy3) was measured before and after addition of 330 nM AflR and after subsequent addition of 1 µM of competitor DNA scaffold. The sample in the cuvette was thoroughly mixed after each addition. DNA and protein concentrations were corrected for dilution (≤6% volume change). All experiments were done at 23°C at least in duplicate, unless otherwise noted.

Stopped-flow measurements

Stopped-flow measurements were conducted at 23ºC using SFM-3000 stopped-flow instrument (BioLogic). The reaction was initiated by mixing 75 µL of protein (20−330 nM AflR concentration after mixing) and 75 µL DNA [20 nM DNA(Cy3) after mixing] in binding buffer. Changes in fluorescence intensity of DNA(Cy3) were measured using excitation wavelength of 546 nm and a 570 nm longpass emission filter. For each concentration of AflR, at least three individual traces were recorded and averaged. A two-phase exponential equation (**Fig. S4F**) was fit to primary stopped flow traces (e.g., **Fig. S4A-D**) to obtain the apparent rate (k_1 or k_2) and amplitude (A_1 or A_2) values at each AflR concentration, respectively. The binding affinity of the DNA(Cy3) scaffold for the first AflR molecule, i.e., the dissociation constant $K_{D,SF}$, was estimated with **Equation 7** from the AflR concentration ([R]) dependence of A_1. The fit parameter A_1^{ind} refers to the value of A_1 at infinite AflR concentration.

$$Y = A_1^{\mathrm{ind}}/(1 + K_{\mathrm{D,SF}}/[R]) \quad \text{Eq.7}$$

Authorship contribution statement

Asmaa Abbas: Conceptualization, Methodology, Formal analysis, Investigation, Writing – original draft, Writing – review & editing, Funding acquisition. **Ranjit K. Prajapati**: Conceptualization, Investigation, Writing – review & editing, Supervision. **Emil Aalto-Setälä**: Methodology, Software, Writing – review & editing. **Alexander A. Baykov**: Conceptualization, Formal analysis, Investigation, Writing – review & editing. **Anssi M. Malinen**: Conceptualization, Formal analysis, Investigation, Writing – review & editing, Funding acquisition, Supervision.

Acknowledgement

Turku Protein Core (TuProtCore) provided access to stopped flow and MicroScale Thermophoresis instruments. Fluorescence scanning of the gels was performed at the Cell Imaging and Cytometry Core, Turku Bioscience Centre, Turku, Finland, with the support of Biocenter Finland.

Data availability

The plasmids, other propagable materials and time-trace data will be available from the corresponding author upon reasonable request.

Competing interests

The authors declare that there are no competing interests associated with the manuscript.

Funding

The work was financially supported by grants from Research Council of Finland [grant numbers 307775, 314100, 335377] and Sigrid Jusélius Foundation to A.M.M., University of Turku Graduate School (UTUGs), Turku University Foundation, and Finnish Cultural Foundation to A.A.

Supplementary materials

Supplementary Methods
Supplementary Figures 1–9

During the preparation of this work the author(s) used ChatGPT 3.5 in order to improve language and readability. After using this tool, the authors reviewed and edited the content as needed and take full responsibility for the content of the publication.

References

[1] G.J.B. Gnonlonfin, K. Hell, Y. Adjovi, P. Fandohan, D.O. Koudande, G.A. Mensah, et al., A review on aflatoxin contamination and its implications in the developing world: a sub-Saharan African perspective, Crit Rev Food Sci Nutr 53 (2013) 349–365. https://doi.org/10.1080/10408398.2010.535718.

[2] M.S. Price, J. Yu, W.C. Nierman, H. Kim, B. Pritchard, C.A. Jacobus, et al., The aflatoxin pathway regulator AflR induces gene transcription inside and outside of the aflatoxin biosynthetic cluster, FEMS Microbiol Lett 255 (2006) 275–279. https://doi.org/10.1111/J.1574-6968.2005.00084.X.

[3] P. Wang, J. Xu, P.-K. Chang, Z. Liu, Q. Kong, New insights of transcriptional regulator AflR in *Aspergillus flavus* physiology, Microbiol Spectr 10 (2022) 00791-21. https://doi.org/10.1128/spectrum.00791-21.

[4] J.E. Flaherty, G.A. Payne, Overexpression of *aflR* leads to upregulation of pathway gene transcription and increased aflatoxin production in *Aspergillus flavus*, Appl Environ Microbiol 63 (1997) 3995–4000. https://doi.org/10.1128/AEM.63.10.3995-4000.1997.

[5] C.P. Woloshuk, K.R. Foutz, J.F. Brewer, D. Bhatnagar, T.E. Cleveland, G.A. Payne, Molecular characterization of *aflR*, a regulatory locus for aflatoxin biosynthesis, Appl Environ Microbiol 60 (1994) 2408–2414. https://doi.org/10.1128/AEM.60.7.2408-2414.1994.

[6] P.K. Chang, K.C. Ehrlich, J. Yu, D. Bhatnagar, T.E. Cleveland, Increased expression of *Aspergillus parasiticus aflR*, encoding a sequence-specific DNA-binding protein, relieves nitrate inhibition of aflatoxin biosynthesis, Appl Environ Microbiol 61 (1995) 2372–2377. https://doi.org/10.1128/AEM.61.6.2372-2377.1995.

[7] P.K. Chang, J. Yu, D. Bhatnagar, T.E. Cleveland, The carboxy-terminal portion of the aflatoxin pathway regulatory protein AFLR of *Aspergillus parasiticus* activates GAL1::lacZ gene expression in *Saccharomyces cerevisiae*, Appl Environ Microbiol 65 (1999) 2508–2512. https://doi.org/10.1128/AEM.65.6.2508-2512.1999.

[8] M. Fernandes, N.P. Keller, T.H. Adams, Sequence-specific binding by *Aspergillus nidulans* AflR, a C6 zinc cluster protein regulating mycotoxin biosynthesis, Mol Microbiol 28 (1998) 1355–1365. https://doi.org/10.1046/J.1365-2958.1998.00907.X.

[9] K.C. Ehrlich, B.G. Montalbano, J.W. Cary, Binding of the C6-zinc cluster protein, AFLR, to the promoters of aflatoxin pathway biosynthesis genes in *Aspergillus parasiticus*, Gene 230 (1999) 249–257. https://doi.org/10.1016/S0378-1119(99)00075-X.

[10] R. Marmorstein, M. Carey, M. Ptashne, S.C. Harrison, DNA recognition by GAL4: structure of a protein-DNA complex, Nature 356 (1992) 408–414. https://doi.org/10.1038/356408a0.

[11] J. Yu, Current understanding on aflatoxin biosynthesis and future perspective in reducing aflatoxin contamination, Toxins, 4 (2012) 1024–1057. https://doi.org/10.3390/TOXINS4111024.

[12] Q. Kong, P.K. Chang, C. Li, Z. Hu, M. Zheng, Q. Sun, et al., Identification of AflR binding sites in the genome of *Aspergillus flavus* by ChIP-Seq, Journal of Fungi, 6 (2020) 52. https://doi.org/10.3390/JOF6020052.

[13] D.M. Meyers, G. Obrian, W.L. Du, D. Bhatnagar, G.A. Payne, Characterization of *aflJ*, a gene required for conversion of pathway intermediates to aflatoxin, Appl Environ Microbiol 64 (1998) 3713–3717. https://doi.org/10.1128/AEM.64.10.3713-3717.1998.

[14] D.R. Georgianna, G.A. Payne, Genetic regulation of aflatoxin biosynthesis: from gene to genome, Fungal Genetics and Biology 46 (2009) 113–125. https://doi.org/10.1016/J.FGB.2008.10.011.

[15] M.G. Amare, N.P. Keller, Molecular mechanisms of *Aspergillus flavus* secondary metabolism and development, Fungal Genetics and Biology 66 (2014) 11–18. https://doi.org/10.1016/J.FGB.2014.02.008.

[16] P.K. Chang, The *Aspergillus parasiticus* protein AFLJ interacts with the aflatoxin pathway-specific regulator AFLR, Molecular Genetics and Genomics 268 (2003) 711–719. https://doi.org/10.1007/S00438-003-0809-3.

[17] K.C. Ehrlich, B.M. Mack, Q. Wei, P. Li, L. V. Roze, F. Dazzo, et al., Association with AflR in endosomes reveals new functions for AflJ in aflatoxin biosynthesis, Toxins 4 (2012) 1582–1600. https://doi.org/10.3390/TOXINS4121582.

[18] P.K. Chang, J.W. Bennett, P.J. Cotty, Association of aflatoxin biosynthesis and sclerotial development in *Aspergillus parasiticus*, Mycopathologia 153 (2002) 41–48. https://doi.org/10.1023/A:1015211915310.

[19] W. Du, G.R. Obrian, G.A. Payne, Function and regulation of *aflJ* in the accumulation of aflatoxin early pathway intermediate in *Aspergillus flavus*, Food Addit Contam 24 (2007) 1043–1050. https://doi.org/10.1080/02652030701513826.

[20] R.P. Sparks, R. Fratti, Use of microscale thermophoresis (MST) to measure binding affinities of components of the fusion machinery, Methods in Molecular Biology 1860 (2019) 191–198. https://doi.org/10.1007/978-1-4939-8760-3_11.

[21] I. Jarmoskaite, I. Alsadhan, P.P. Vaidyanathan, D. Herschlag, How to measure and evaluate binding affinities, Elife 9 (2020) 1–34. https://doi.org/10.7554/ELIFE.57264.

[22] H. Hwang, S. Myong, Protein induced fluorescence enhancement (PIFE) for probing protein–nucleic acid interactions, Chem Soc Rev 43 (2014) 1221–1229. https://doi.org/10.1039/C3CS60201J.

[23] Q. Kong, C. Chi, J. Yu, S. Shan, Q. Li, Q. Li, et al., The inhibitory effect of *Bacillus megaterium* on aflatoxin and cyclopiazonic acid biosynthetic pathway gene expression in *Aspergillus flavus*, Appl Microbiol Biotechnol 98 (2014) 5161–5172. https://doi.org/10.1007/S00253-014-5632-8.

[24] S. Kumar, G. Stecher, K. Tamura, MEGA7: molecular evolutionary genetics analysis version 7.0 for bigger datasets, Mol Biol Evol 33 (2016) 1870. https://doi.org/10.1093/MOLBEV/MSW054.

[25] B.H. Liu, J.F. Brewer, J.E. Flaherty, G. Payne, D. Bhatnagar, F.S. Chu, Immunochemical identification of AFLR, a regulatory protein, involved in aflatoxin biosynthesis, Food Agric Immunol 9 (1997) 289–298. https://doi.org/10.1080/09540109709354959.

[26] P. Rice, L. Longden, A. Bleasby, EMBOSS: The European molecular biology open software suite, Trends in Genetics 16 (2000) 276–277. https://doi.org/10.1016/S0168-9525(00)02024-2.

[27] C.Z. Lee, G.Y. Liou, G.F. Yuan, Comparison of the *aflR* gene sequences of strains in *Aspergillus* section *Flavi*, Microbiology (N Y) 152 (2006) 161–170. https://doi.org/10.1099/MIC.0.27618-0.

[28] P.K. Chang, L.L. Scharfenstein, B. Mack, Q. Wei, M. Gilbert, M. Lebar, et al., Identification of a copper-transporting ATPase involved in biosynthesis of *A. flavus* conidial pigment, Appl Microbiol Biotechnol 103 (2019) 4889–4897. https://doi.org/10.1007/S00253-019-09820-0.

[29] T. Jin, W. Chuenchor, J. Jiang, J. Cheng, Y. Li, K. Fang, et al., Design of an expression system to enhance MBP-mediated crystallization, Scientific Reports 7 (2017) 1–11. https://doi.org/10.1038/srep40991.

[30] S.P. Romero-Pérez, A.A. Covarrubias, F. Campos, A simple method to purify intrinsically disordered proteins by adjusting trichloroacetic acid concentration, Protein Expr Purif 202 (2023) 106183. https://doi.org/10.1016/J.PEP.2022.106183.

[31] T. Mahmood, P.C. Yang, Western blot: technique, theory, and troubleshooting, N Am J Med Sci 4 (2012) 429. https://doi.org/10.4103/1947-2714.100998.

[32] A. Langer, T. Bartoschik, O. Cehlar, S. Duhr, P. Baaske, W. Streicher, A New spectral shift-based method to characterize molecular interactions, Assay Drug Dev Technol 20 (2022) 83. https://doi.org/10.1089/ADT.2021.133.

[33] L. Hellinen, S. Bahrpeyma, A.K. Rimpelä, M. Hagström, M. Reinisalo, A. Urtti, Microscale thermophoresis as a screening tool to predict melanin binding of drugs, Pharmaceutics 12 (2020) 554. https://doi.org/10.3390/PHARMACEUTICS12060554.

Supplementary material:

Supplementary Methods
Supplementary Figures S1–S9

Supplementary Methods

Purification of MBP

Frozen *E. coli* BL21(DE3) cells (containing pAM074 plasmid for MBP expression) were re-suspended in cell lysis buffer S (50 mM Tris-HCl, pH 7.9, 0.5 M KCl, 5% glycerol, 1 mM β-mercaptoethanol, 20 µM ZnSO4) supplemented with 0.1 mM PMSF. The cells were then disrupted by sonication (5 times of 30 s, with 5 min of incubations on ice in between). The lysate was cleared by centrifugation at 39,000 g for 30 min at 4°C. Proteins in the supernatant were precipitated by slowly adding solid ammonium sulfate to final concentration of 300 g/L, incubated on ice for 30 min, and centrifuged at 12,000 g for 25 min at 4°C. The supernatant was discarded, and the pellet (i.e, ammonium sulfate precipitate), was re-suspended in 25 mL of cell lysis buffer S followed by centrifugation at 20,400 g for 10 min at 4°C to remove non-dissolved particles. The supernatant was filtered through a 0.2 µm syringe filter and loaded at a flow rate of 0.5 mL/min onto an MBPTrap HP column (1 mL column, GE Healthcare), which had been pre-equilibrated with lysis buffer S. The column was then washed with 5 mL of lysis buffer S followed by the elution of MBP with 5 mL of 20 mM maltose in lysis buffer S. MBP was concentrated to a final volume of about 0.2 mL using Amicon® Ultra-4 centrifugal filter, aliquoted and stored at -80ºC.

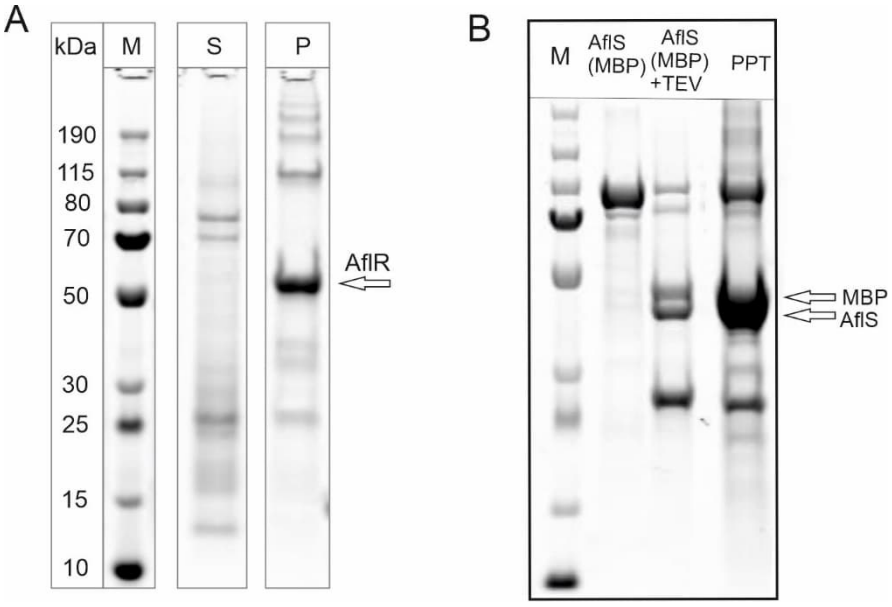

Figure S1. Expression and purification of AflR and AflS(MBP) proteins. (A) SDS-PAGE analysis of purified AflR following expression in *Escherichia coli* T7 Express at 37°C for 3 hours. AflR was found in the inclusion bodies, with a distinct 50 kDa band corresponding to AflR in the precipitate. M denotes the protein marker, S represents the supernatant, and P indicates the precipitate. (B) Removal of the fusion tag MBP was achieved by incubating AflS(MBP) with TEV protease. SDS-PAGE analysis of the soluble and non-soluble fractions (supernatant and precipitate) revealed precipitation of AflS (PPT fraction) upon incubation with TEV.

$K_{D,S\text{-}R}$ (nM)	F_S	F_{SR}
23.8±5.9	103.7±3.2	186.9±2.7

Parameters are reported with their standard error.

Figure S2. Best-fit parameters of AflR-AflS interaction assay data in Figure 2A.

A

Table. Best-fit parameters of competitor experiments in Figure 4C and S2B

Labelled scaffold	Competitor	t_1 (s)	$\|A_1\|$	t_2 (s)	$\|A_2\|$	y_0
DNA(FAM)	wild-type	51±7	1.7±0.1	575±16	8.9±0.1	60.9±0.1
DNA(FAM)	ΔT1	641±45	1.9±0.1	n.a.	n.a.	52.7±0.1
DNA(FAM)	L+1	63±5	2.4±0.1	819±64	5.4±0.1	57.7±0.2
DNA(Cy3)	wild-type	45±7	4.0±0.1	604±12	9.7±0.1	43.4±0.1

1-phase exponential equation:

$y = A_1 * e^{-x/t_1} + y_0$

2-phase exponential equation:

$y = A_1 * e^{-x/t_1} + A_2 * e^{-x/t_2} + y_0$

The DNA(FAM) + ΔT1 comptitor experiment data were fit with a 1-phase exponential equation, whereas other data were fit using a 2-phase exponential equation.

B

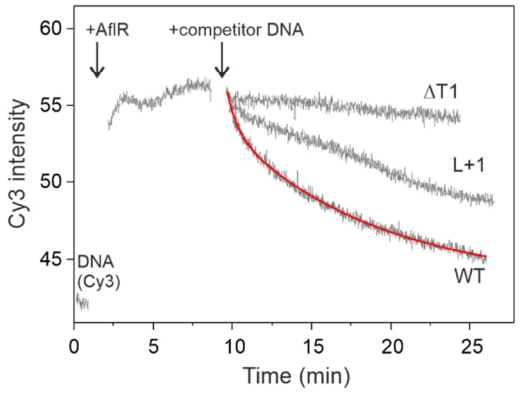

C

Table. Best-fit parameters for the equilbrium binding of AflR to DNA(Cy3) in Fig. 5

Competitor	$K_{1,DNA(Cy3)}$ (μM^2)	F_∞	F_0
wild-type	0.23±0.2	92.8±0.5	63.9±0.6

Fit equation:

$y = (F_\infty + F_0 K_{1,DNA(Cy3)} / [R]^2) / (1 + K_{1,DNA(Cy3)} / [R]^2)$

Figure S3. Kinetics of AflR·DNA complex formation and stability**.** (A) Best-fit parameters of competition experiments in Figure 4C and S3B. (B) The fluorescence intensity increased after AflR addition, indicating the formation of AflR·DNA(Cy3) complex. The addition of WT, L+1 or ΔT1 competitor DNA caused full or partial disruption of AflR·DNA(Cy3) complexes, as indicated by the gradual decrease in intensity. The lifetime of the AflR·DNA(Cy3) complex was estimated by fitting 1- or 2-phase exponential decay equations to the dissociation part, i.e. the fluorescence increase after ~10 min, of the reaction progress curves. Fit curve is shown in red, and parameters are shown in Figure S3A. (C) Best-fit parameters for the equilibrium binding of AflR to DNA(Cy3) in Figure 5. The fit parameter $K_{1,DNA(Cy3)}$ is the product of two dissociation constants governing the binding of two AflR molecules to one DNA(Cy3) molecule. Parameters F_0 and F_∞ refer to the fluorescence intensity of DNA(Cy3) in the absence of AflR and at infinite AflR concentration, respectively. [R] is the AflR concentration.

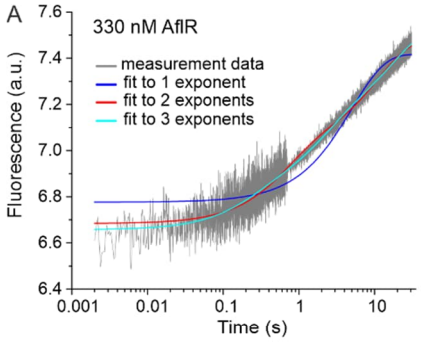

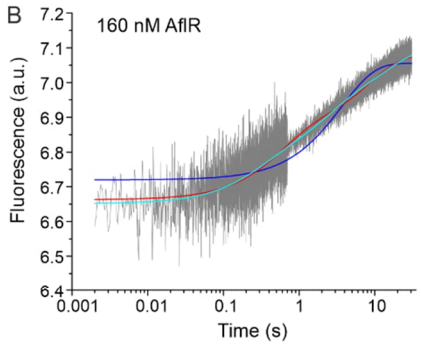

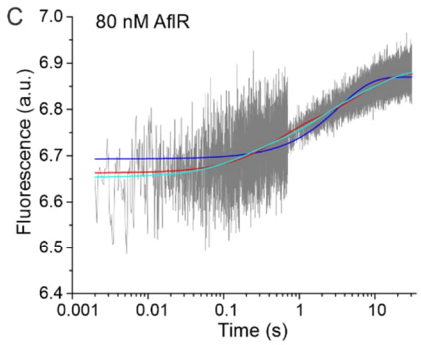

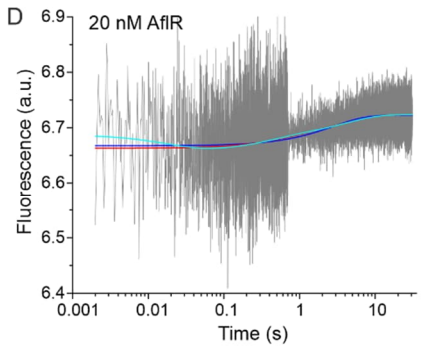

E

1-phase exponential: $y = A_1e^{-x/t_1} + y_0$

2-phase exponential: $y = A_1e^{-x/t_1} + A_2e^{-x/t_2} + y_0$

3-phase exponential: $y = A_1e^{-x/t_1} + A_2e^{-x/t_2} + A_3e^{-x/t_3} + y_0$

t to k conversion: $k_n = 1 / t_n$

* in the above equations x is time, y is measured fluorescence, A_n is the amplitude of reaction phase n, t_n is lifetime of the reaction phase n, and y_n is the end-point fluorescence.

F Table. Residual sum of square for the fits to 1-3 phase exponential decay equations

[AflR] (nM)	Number of exponential phases		
	1	2	3
330	47.77	21.97	20.90
160	29.33	21.17	20.89
80	22.01	20.07	19.97
20	32.06	32.00	31.96

G Table. Best-fit parameters of 2-phase exponential decay equation

[AflR] (nM)	k_1 (s^{-1})	$-A_1$	k_2 (s^{-1})	$-A_2$	y_0
330	1.49±0.02	0.326±0.002	0.091±0.001	0.471±0.001	7.48±0.01
160	1.79±0.04	0.194±0.002	0.119±0.002	0.222±0.002	6.88±0.01
80	2.08±0.09	0.095±0.002	0.150±0.004	0.121±0.002	7.08±0.01
20	1.56±0.50	0.022±0.005	0.235±0.033	0.039±0.005	7.48±0.01

H

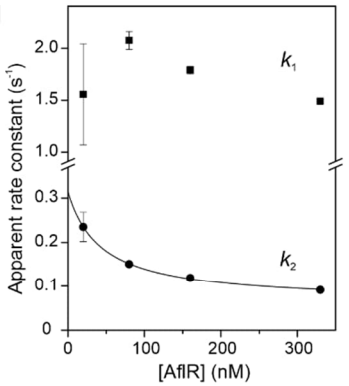

I Table. Best-fit parameters of Eq. 7 to k_{app} and A_1^{app} data in Fig. 6D

$K_{D,SF}$ (nM)	A_1^{ind}
816±246	1.14±0.26

Parameters are reported with their standard error.

Figure S4. Stopped-flow traces with 1-(purple), 2-(red), and 3-(green) phase exponential fits and their best-fitting parameters. (A) Fluorescence intensity of DNA(Cy3) after mixing with 330 nM AflR. (B) Fluorescence intensity of DNA(Cy3) after mixing with 160 nM AflR. (C) Fluorescence intensity of DNA(Cy3) after mixing with 80 nM AflR. (D) Fluorescence intensity of DNA(Cy3) after mixing with 20 nM AflR. (E) Equations of 1-, 2-, and 3-phase exponential equations. In the equations x represents time, y represents measured fluorescence, A_n represents the amplitude of reaction phase n, t_n represents the lifetime of the reaction phase n, and y_n represents the end-point fluorescence. (F) Table shows the residual sum of squares for the fits to 1-3 phase exponential equations. (G) The best-

fit parameters of 2-phase exponential equation. (H) Same as Fig. 6C but the ordinate is shown in linear scale with a break. (I) The best-fit parameters of Eq. 7 to A_{app} data in Fig. 6D.

A

-291

CGGCTCGTATGTTGTGT**G**TAGATTACATGCTTATACTCTTATGCGAGAGGAAGAGATCACAATTGATCTGATA
TTACGACTACAAGAATAGCGGTGACATCCAGCATGCGTATCTTGCCAATGGGTGAGCTATCGAACTAATTGGC
CCACCGGGCTTTCGGAAAGCGATCAGCTTGTAAGGCATTCTAGCGACTTTGACTTTATCTATTATAAACTGTG
AATAAATATTCTAGCTGGTTGCAACTTTTTAACTTCCTACAAACTCCTTCTGCCGTCTATAGTCAACAAACAC
CACAGGAACAGCAATC**A**TGGTTCTCCCTACTGCCCCAGAG**C**AGTTGAAGACAAGTTCGCTGGCGTTACCCAA**A**C
TTAA **+1** **+25**
*

B

CGGCTCGTATGTTGTGTGGAATTGTGAGCGGATAACAATTTCACACAGGAAACAGCTATGACATGATTACGAA
TTCGAGCTCTATTCCAATGCGCTTAACGAATCAAACCTGCCAGCCCATTTAGATCAAAAGAAGATCACACCTG
TATGGACAAAGTTTGGACTCTTAAGAGTCTCGGTATCATACAGACGTGATTGGAAGTTTGAAATTAACAATAC
AAACGACGAATTATTTTCAGCTCGACATGCATCTGTCTCACATAACTCACAAGGACCCCAGAATCAGCCAGAA
CAAGAAGGACAAAGTGATCAAGACATAGGGAAACGCCAACCACAATTTCAACAGCAGCAGCAGCCCCAACAGC
AGCAGCAGCAGCAGCAACAGCAACAGAGACAACACCAGGTCCAGACACAACAACAAAGACAGATACCTGATAG
GAGAAGCTTGGCACTGGCCGTCGTTTTACAACGTCGTGACTGGGAAAACCCTGGCGTTACCCAA**A**CTTAA
*

C

```
Forward primer (EAS013): 5'-CGGCTCGTATGTTGTGTG-3’

Reverse primer (EAS054): 5'-TTAAGTTGGGTAACGCCAG-3’
                                  *
```

Figure S5. Sequences of DNA fragments used in EMSA assays. (A) *norA* promoter fragment contained *norA* sequence (shown in black font) from position -291 to +25 relative to the translation start site at +1 (these residues are numbered and shown in bold). The fragment also includes flanking sequences (shown in red font) with primer binding sites (indicated with underline). The top strand sequence is shown. Atto488 was attached to the bottom strand T residue via a C6 linker in a location indicated with an asterisk. The AflR binding motif is highlighted with a rectangle. (B) The sequence of the negative control DNA is shown similarly. The sequence shown in black font is from the *Saccharomyces cerevisiae* gene *ATG13*, while the red sequence derives from the template plasmid pAM041 (based on pUC18). (C) The sequences of the forward and reverse primers used to PCR amplify the *norA* promoter or negative control DNA fragments, respectively. The Atto488 attachment site in the reverse primer is indicated with an asterisk.

>pAM041
CGGGTTGGACTCAAGACGATAGTTACCGGATAAGGCGCAGCGGTCGGGCTGAACGGGGGGTTCGTGCACACAGCCCAGCTTGGAGCGAACGACCTACACCGAACTGAGATACCT
ACAGCGTGAGCTTTGAGAAAGCGCCACGCTTCCCGAAGGGAGAAAGGCGGACAGGTATCCGGTAAGCGGCAGGGTCGGAACAGGAGAGCGCACGAGGGAGCTTCCAGGGGGAAA
CGCCTGGTATCTTTATAGTCCTGTCGGGTTTCGCCACCTCTGACTTGAGCGTCGATTTTTGTGATGCTCGTCAGGGGGGCGGAGCCTATGGAAAAACGCCAGCAACGCGGCCTT
TTTACGGTTCCTGGCCTTTTGCTGGCCTTTTGCTCACATGTTCTTTCCTGCGTTATCCCCTGATTCTGTGGATAACCGTATTACCGCCTTTGAGTGAGCTGATACCGCTCGCCG
CAGCCGAACGACCGAGCGCAGCGAGTCAGTGAGCGAGGAAGCGGAAGAGCGCCCAATACGCAAACCGCCTCTCCCCGCGCGTTGGCCGATTCATTAATGCAGCTGGCACGACAG
GTTTCCCGACTGGAAAGCGGGCAGTGAGCGCAACGCAATTAATGTGAGTTAGCTCACTCATTAGGCACCCCAGGCTTTACACTTTATGCTTCCGGCTCGTATGTTGTGTGGAAT
TGTGAGCGGATAACAATTTCACACAGGAAACAGCTATGACATGATTACGAATTCGAGCTCTATTCCAATGCGCTTAACGAATCAAACCTGCCAGCCCATTTAGATCAAAAGAAG
ATCACACCTGTATGGACAAAGTTTGGACTCTTAAGAGTCTCGGTATCATACAGACGTGATTGGAAGTTTGAAATTAACAATACAAACGACGAATTATTTTCAGCTCGACATGCA
TCTGTCTCACATAACTCACAAGGACCCCAGAATCAGCCAGAACAAGAAGGACAAAGTGATCAAGACATAGGGAAACGCCAACCACAATTTCAACAGCAGCAGCAGCCCCAACAG
CAGCAGCAGCAGCAGCAACAGCAACAGAGACAACACCAGGTCCAGACACAACAACAAAGACAGATACCTGATAGGAGAAGCTTGGCACTGGCCGTCGTTTTACAACGTCGTGAC
TGGGAAAACCCTGGCGTTACCCAACTTAATCGCCTTGCAGCACATCCCCCTTTCGCCAGCTGGCGTAATAGCGAAGAGGCCCGCACCGATCGCCCTTCCCAACAGTTGCGCAGC
CTGAATGGCGAATGGCGCCTGATGCGGTATTTTCTCCTTACGCATCTGTGCGGTATTTCACACCGCATATGGTGCACTCTCAGTACAATCTGCTCTGATGCCGCATAGTTAAGC
CAGCCCCGACACCCGCCAACACCCGCTGACGCGCCCTGACGGGCTTGTCTGCTCCCGGCATCCGCTTACAGACAAGCTGTGACCGTCTCCGGGAGCTGCATGTGTCAGAGGTTT
TCACCGTCATCACCGAAACGCGCGAGACGAAAGGGCCTCGTGATACGCCTATTTTTATAGGTTAATGTCATGATAATAATGGTTTCTTAGACGTCAGGTGGCACTTTTCGGGGA
AATGTGCGCGGAACCCCTATTTGTTTATTTTTCTAAATACATTCAAATATGTATCCGCTCATGAGACAATAACCCTGATAAATGCTTCAATAATATTGAAAAAGGAAGAGTATG
AGTATTCAACATTTCCGTGTCGCCCTTATTCCCTTTTTTGCGGCATTTTGCCTTCCTGTTTTTGCTCACCCAGAAACGCTGGTGAAAGTAAAAGATGCTGAAGATCAGTTGGGT
GCACGAGTGGGTTACATCGAACTGGATCTCAACAGCGGTAAGATCCTTGAGAGTTTTCGCCCCGAAGAACGTTTTCCAATGATGAGCACTTTTAAAGTTCTGCTATGTGGCGCG
GTATTATCCCGTATTGACGCCGGGCAAGAGCAACTCGGTCGCCGCATACACTATTCTCAGAATGACTTGGTTGAGTACTCACCAGTCACAGAAAAGCATCTTACGGATGGCATG
ACAGTAAGAGAATTATGCAGTGCTGCCATAACCATGAGTGATAACACTGCGGCCAACTTACTTCTGACAACGATCGGAGGACCGAAGGAGCTAACCGCTTTTTTGCACAACATG
GGGGATCATGTAACTCGCCTTGATCGTTGGGAACCGGAGCTGAATGAAGCCATACCAAACGACGAGCGTGACACCACGATGCCTGTAGCAATGGCAACAACGTTGCGCAAACTA
TTAACTGGCGAACTACTTACTCTAGCTTCCCGGCAACAATTAATAGACTGGATGGAGGCGGATAAAGTTGCAGGACCACTTCTGCGCTCGGCCCTTCCGGCTGGCTGGTTTATT
GCTGATAAATCTGGAGCCGGTGAGCGTGGGTCTCGCGGTATCATTGCAGCACTGGGGCCAGATGGTAAGCCCTCCCGTATCGTAGTTATCTACACGACGGGGAGTCAGGCAACT
ATGGATGAACGAAATAGACAGATCGCTGAGATAGGTGCCTCACTGATTAAGCATTGGTAACTGTCAGACCAAGTTTACTCATATATACTTTAGATTGATTTAAAACTTCATTTT
TAATTTAAAAGGATCTAGGTGAAGATCCTTTTTGATAATCTCATGACCAAAATCCCTTAACGTGAGTTTTCGTTCCACTGAGCGTCAGACCCCGTAGAAAAGATCAAAGGATCT
TCTTGAGATCCTTTTTTTCTGCGCGTAATCTGCTGCTTGCAAACAAAAAAACCACCGCTACCAGCGGTGGTTTGTTTGCCGGATCAAGAGCTACCAACTCTTTTTCCGAAGGTA
ACTGGCTTCAGCAGAGCGCAGATACCAAATACTGTTCTTCTAGTGTAGCCGTAGTTAGGCCACCACTTCAAGAACTCTGTAGCACCGCCTACATACCTCGCTCTGCTAATCCTG
TTACCAGTGGCTGCTGCCAGTGGCGATAAGTCGTGTCTTAC

Figure S6. Sequence of plasmid pAM041. The plasmid was used to PCR amplify the negative control DNA for the EMSA assays, using primers EAS013 and EAS054. The negative control DNA is from the *S. cerevisiae* gene ATG13.

>pAM068
CGATCCCGCGAAATTAATACGACTCACTATAGGGGAATTGTGAGCGGATAACAATTCCCCTCTAGAAATAATTTTGTTTAACTTTAAGAAGGAGATATACCATGGGGTCAAGTC
ACCATCACCACCACCACGAGAACTTATACTTTCAGGGTCATATGGTTGATCACATTTCCCCTCGTGCCAGTCCGGGCCCCATCCGTTCATCGCAAACCCGTCGTGCGCGTAAGT
TACGCGACTCGTGCACTAGTTGCGCATCAAGTAAGGTACGTTGCACGAAAGAAAAGCCCGCATGTGCGCGCTGCATCGAACGTGGCCTGGCTTGTCAGTATATGGTCAGCAAAC
GTATGGGCCGCAATCCCCGTGCCCCGAGCCCACTGGATTCAACGCGCCGTCCGTCAGAGAGCTTGCCCAGCGCACGCTCGGAACAAGGATTACCTGCACACAACACCTACTCCA
CCCCGCACGCCCATACCCAGGCACATACGCATGCACATAGTCACCCGCAGCCCCATCCACAATCCCACCCGCAGAGCAATCAGCCACCGCATGCATTACCAACTCCGAACGGCT
CGTCCTCTGTGTCCGCAATCTTTTCACACCAGAGTCCGCCGCCACCGGTGGAAACACAGGGCCTTGGTGGCGACTTGGCCGGTCAGGAACAAAGTACGCTGTCGTCTCTGACCG
TGGACAGTGAGTTCGGTGGTAGCCTGCAGAGTATGGAGCACGGCAATCACGCGGATTTTCTCGCAGAGAGCACAGGAAGCCTGTTCGACGCATTCTTAGAGGTTGGTACACCGA
TGATCGACCCGTTTCTCGAAAGCGCACCATTGCCGCCTTTCCAGGCACGCTATTGCTGTTTCTCACTGGCCCTGCAGACACTCACACACCTGTTCCCTCACGCTCCCTTGGGAT
GTCAACTGCGTTTAACTGACGGCGAGGATTCTTCGTGCAATTTAATGACTACTGATATGGTCATCTCGGGGAATAAGCGTGCGACTGATGCGGTGCGTAAAATCCTCGGCTGTA
GCTGCGCGCAGGATGGGTACCTGTTAAGCATGGTCGTTCTCATCGTTTTAAAGGTGCTGGCCTGGTATGCCGCAGCAGCGGGGACCCAATGTACCTCTACTGCAGCCGGTGGAG
AGACCAATTCCGGCAGCTGCTCGAACTCCCCAGCCACGGTAAGCTCTGGATGTCTGACCGAAGAGCGCGTTCTCCACCTTCCCTCGATGATGGGCGAGGACTGCGTAGACGAAG
AAGATCAGCCGCGTGTTGCAGCGCAGCTGGTTCTGAGCGAGTTGCACCGTGTACAGTCACTTGTTAATCTGCTCGCCAAGCGTCTGCAAGAAGGCGGAGATGATGCCGCTGGGA
TTCCTGCCCATCACCCGGCGAGCCCGTTCTCGCTGTTGGGGTTTTCAGGCCTCGAAGCGAACCTGCGTCATCGTCTTCGCGCAGTGAGCTCGGACATTATCGATTATCTGCATC
GCGAGTGAGAATTCCTCGAGCACCACCACCACCACCACTGAGATCCGGCTGCTAACAAAGCCCGAAAGGAAGCTGAGTTGGCTGCTGCCACCGCTGAGCAATAACTAGCATAAC
CCCTTGGGGCCTCTAAACGGGTCTTGAGGGGTTTTTTGCTGAAAGGAGGAACTATATCCGGATTGGCGAATGGGACGCGCCCTGTAGCGGCGCATTAAGCGCGGCGGGTGTGGT
GGTTACGCGCAGCGTGACCGCTACACTTGCCAGCGCCCTAGCGCCCGCTCCTTTCGCTTTCTTCCCTTCCTTTCTCGCCACGTTCGCCGGCTTTCCCCGTCAAGCTCTAAATCG
GGGGCTCCCTTTAGGGTTCCGATTTAGTGCTTTACGGCACCTCGACCCCAAAAAACTTGATTAGGGTGATGGTTCACGTAGTGGGCCATCGCCCTGATAGACGGTTTTTCGCCC
TTTGACGTTGGAGTCCACGTTCTTTAATAGTGGACTCTTGTTCCAAACTGGAACAACACTCAACCCTATCTCGGTCTATTCTTTTGATTTATAAGGGATTTTGCCGATTTCGGC
CTATTGGTTAAAAAATGAGCTGATTTAACAAAAATTTAACGCGAATTTTAACAAAATATTAACGCTTACAATTTAGGTGGCACTTTTCGGGGAAATGTGCGCGGAACCCCTATT
TGTTTATTTTTCTAAATACATTCAAATATGTATCCGCTCATGAGACAATAACCCTGATAAATGCTTCAATAATATTGAAAAAGGAAGAGTATGAGTATTCAACATTTCCGTGTC
GCCCTTATTCCCTTTTTTGCGGCATTTTGCCTTCCTGTTTTTGCTCACCCAGAAACGCTGGTGAAAGTAAAAGATGCTGAAGATCAGTTGGGTGCACGAGTGGGTTACATCGAA
CTGGATCTCAACAGCGGTAAGATCCTTGAGAGTTTTCGCCCCGAAGAACGTTTTCCAATGATGAGCACTTTTAAAGTTCTGCTATGTGGCGCGGTATTATCCCGTATTGACGCC
GGGCAAGAGCAACTCGGTCGCCGCATACACTATTCTCAGAATGACTTGGTTGAGTACTCACCAGTCACAGAAAAGCATCTTACGGATGGCATGACAGTAAGAGAATTATGCAGT
GCTGCCATAACCATGAGTGATAACACTGCGGCCAACTTACTTCTGACAACGATCGGAGGACCGAAGGAGCTAACCGCTTTTTTGCACAACATGGGGGATCATGTAACTCGCCTT
GATCGTTGGGAACCGGAGCTGAATGAAGCCATACCAAACGACGAGCGTGACACCACGATGCCTGCAGCAATGGCAACAACGTTGCGCAAACTATTAACTGGCGAACTACTTACT
CTAGCTTCCCGGCAACAATTAATAGACTGGATGGAGGCGGATAAAGTTGCAGGACCACTTCTGCGCTCGGCCCTTCCGGCTGGCTGGTTTATTGCTGATAAATCTGGAGCCGGT
GAGCGTGGGTCTCGCGGTATCATTGCAGCACTGGGGCCAGATGGTAAGCCCTCCCGTATCGTAGTTATCTACACGACGGGGAGTCAGGCAACTATGGATGAACGAAATAGACAG
ATCGCTGAGATAGGTGCCTCACTGATTAAGCATTGGTAACTGTCAGACCAAGTTTACTCATATATACTTTAGATTGATTTAAAACTTCATTTTTAATTTAAAAGGATCTAGGTG
AAGATCCTTTTTGATAATCTCATGACCAAAATCCCTTAACGTGAGTTTTCGTTCCACTGAGCGTCAGACCCCGTAGAAAAGATCAAAGGATCTTCTTGAGATCCTTTTTTTCTG
CGCGTAATCTGCTGCTTGCAAACAAAAAAACCACCGCTACCAGCGGTGGTTTGTTTGCCGGATCAAGAGCTACCAACTCTTTTTCCGAAGGTAACTGGCTTCAGCAGAGCGCAG
ATACCAAATACTGTCCTTCTAGTGTAGCCGTAGTTAGGCCACCACTTCAAGAACTCTGTAGCACCGCCTACATACCTCGCTCTGCTAATCCTGTTACCAGTGGCTGCTGCCAGT
GGCGATAAGTCGTGTCTTACCGGGTTGGACTCAAGACGATAGTTACCGGATAAGGCGCAGCGGTCGGGCTGAACGGGGGGTTCGTGCACACAGCCCAGCTTGGAGCGAACGACC
TACACCGAACTGAGATACCTACAGCGTGAGCTATGAGAAAGCGCCACGCTTCCCGAAGGGAGAAAGGCGGACAGGTATCCGGTAAGCGGCAGGGTCGGAACAGGAGAGCGCACG
AGGGAGCTTCCAGGGGGAAACGCCTGGTATCTTTATAGTCCTGTCGGGTTTCGCCACCTCTGACTTGAGCGTCGATTTTTGTGATGCTCGTCAGGGGGGCGGAGCCTATGGAAA
AACGCCAGCAACGCGGCCTTTTTACGGTTCCTGGCCTTTTGCTGGCCTTTTGCTCACATGTTCTTTCCTGCGTTATCCCCTGATTCTGTGGATAACCGTATTACCGCCTTTGAG
TGAGCTGATACCGCTCGCCGCAGCCGAACGACCGAGCGCAGCGAGTCAGTGAGCGAGGAAGCGGAAGAGCGCCTGATGCGGTATTTTCTCCTTACGCATCTGTGCGGTATTTCA
CACCGCAATGGTGCACTCTCAGTACAATCTGCTCTGATGCCGCATAGTTAAGCCAGTATACACTCCGCTATCGCTACGTGACTGGGTCATGGCTGCGCCCCGACACCCGCCAAC
ACCCGCTGACGCGCCCTGACGGGCTTGTCTGCTCCCGGCATCCGCTTACAGACAAGCTGTGACCGTCTCCGGGAGCTGCATGTGTCAGAGGTTTTCACCGTCATCACCGAAACG
CGCGAGGCAGCTGCGGTAAAGCTCATCAGCGTGGTCGTGAAGCGATTCACAGATGTCTGCCTGTTCATCCGCGTCCAGCTCGTTGAGTTTCTCCAGAAGCGTTAATGTCTGGCT
TCTGATAAAGCGGGCCATGTTAAGGGCGGTTTTTTCCTGTTTGGTCACTGATGCCTCCGTGTAAGGGGGATTTCTGTTCATGGGGGTAATGATACCGATGAAACGAGAGAGGAT
GCTCACGATACGGGTTACTGATGATGAACATGCCCGGTTACTGGAACGTTGTGAGGGTAAACAACTGGCGGTATGGATGCGGCGGGACCAGAGAAAAATCACTCAGGGTCAATG
CCAGCGCTTCGTTAATACAGATGTAGGTGTTCCACAGGGTAGCCAGCAGCATCCTGCGATGCAGATCCGGAACATAATGGTGCAGGGCGCTGACTTCCGCGTTTCCAGACTTTA
CGAAACACGGAAACCGAAGACCATTCATGTTGTTGCTCAGGTCGCAGACGTTTTGCAGCAGCAGTCGCTTCACGTTCGCTCGCGTATCGGTGATTCATTCTGCTAACCAGTAAG
GCAACCCCGCCAGCCTAGCCGGGTCCTCAACGACAGGAGCACGATCATGCGCACCCGTGGGGCCGCCATGCCGGCGATAATGGCCTGCTTCTCGCCGAAACGTTTGGTGGCGGG
ACCAGTGACGAAGGCTTGAGCGAGGGCGTGCAAGATTCCGAATACCGCAAGCGACAGGCCGATCATCGTCGCGCTCCAGCGAAAGCGGTCCTCGCCGAAAATGACCCAGAGCGC
TGCCGGCACCTGTCCTACGAGTTGCATGATAAAGAAGACAGTCATAAGTGCGGCGACGATAGTCATGCCCCGCGCCCACCGGAAGGAGCTGACTGGGTTGAAGGCTCTCAAGGG
CATCGGTCGAGATCCCGGTGCCTAATGAGTGAGCTAACTTACATTAATTGCGTTGCGCTCACTGCCCGCTTTCCAGTCGGGAAACCTGTCGTGCCAGCTGCATTAATGAATCGG
CCAACGCGCGGGGAGAGGCGGTTTGCGTATTGGGCGCCAGGGTGGTTTTTCTTTTCACCAGTGAGACGGGCAACAGCTGATTGCCCTTCACCGCCTGGCCCTGAGAGAGTTGCA
GCAAGCGGTCCACGCTGGTTTGCCCCAGCAGGCGAAAATCCTGTTTGATGGTGGTTAACGGCGGGATATAACATGAGCTGTCTTCGGTATCGTCGTATCCCACTACCGAGATAT
CCGCACCAACGCGCAGCCCGGACTCGGTAATGGCGCGCATTGCGCCCAGCGCCATCTGATCGTTGGCAACCAGCATCGCAGTGGGAACGATGCCCTCATTCAGCATTTGCATGG
TTTGTTGAAAACCGGACATGGCACTCCAGTCGCCTTCCCGTTCCGCTATCGGCTGAATTTGATTGCGAGTGAGATATTTATGCCAGCCAGCCAGACGCAGACGCGCCGAGACAG
AACTTAATGGGCCCGCTAACAGCGCGATTTGCTGGTGACCCAATGCGACCAGATGCTCCACGCCCAGTCGCGTACCGTCTTCATGGGAGAAAATAATACTGTTGATGGGTGTCT
GGTCAGAGACATCAAGAAATAACGCCGGAACATTAGTGCAGGCAGCTTCCACAGCAATGGCATCCTGGTCATCCAGCGGATAGTTAATGATCAGCCCACTGACGCGTTGCGCGA
GAAGATTGTGCACCGCCGCTTTACAGGCTTCGACGCCGCTTCGTTCTACCATCGACACCACCACGCTGGCACCCAGTTGATCGGCGCGAGATTTAATCGCCGCGACAATTTGCG
ACGGCGCGTGCAGGGCCAGACTGGAGGTGGCAACGCCAATCAGCAACGACTGTTTGCCCGCCAGTTGTTGTGCCACGCGGTTGGGAATGTAATTCAGCTCCGCCATCGCCGCTT
CCACTTTTTCCCGCGTTTTCGCAGAAACGTGGCTGGCCTGGTTCACCACGCGGGAAACGGTCTGATAAGAGACACCGGCATACTCTGCGACATCGTATAACGTTACTGGTTTCA
CATTCACCACCCTGAATTGACTCTCTTCCGGGCGCTATCATGCCATACCGCGAAAGGTTTTGCGCCATTCGATGGTGTCCGGGATCTCGACGCTCTCCCTTATGCGACTCCTGC
ATTAGGAAGCAGCCCAGTAGTAGGTTGAGGCCGTTGAGCACCGCCGCCGCAAGGAATGGTGCATGCAAGGAGATGGCGCCCAACAGTCCCCCGGCCACGGGGCCTGCCACCATA
CCCACGCCGAAACAAGCGCTCATGAGCCCGAAGTGGCGAGCCCGATCTTCCCCATCGGTGATGTCGGCGATATAGGCGCCAGCAACCGCACCTGTGGCGCCGGTGATGCCGGCC
ACGATGCGTCCGGCGTAGAGGATCGAGATCT

Figure S7. Sequence of plasmid pAM068. The plasmid was used to express *Aspergillus flavus* AflR.

>pAM073
CGATCCCGCGAAATTAATACGACTCACTATAGGGGAATTGTGAGCGGATAACAATTCCCCTCTAGAAATAATTTTGTTTAACTTTAAGAAGGAGATATACCATGGGGAGTCACCATCACCACC
ACCACGAAGAAGGTAAACTGGTAATCTGGATTAACGGCGATAAAGGCTATAACGGTCTCGCTGAAGTCGGTAAGAAATTCGAGAAAGATACCGGAATTAAAGTCACCGTTGAGCATCCGGATA
AACTGGAAGAGAAATTCCCACAGGTTGCGGCAACTGGCGATGGCCCTGACATTATCTTCTGGGCACACGACCGCTTTGGTGGCTACGCTCAATCTGGCCTGTTGGCTGAAATCACCCCGGACA
AAGCGTTCCAGGACAAGCTGTATCCGTTTACCTGGGATGCCGTACGTTACAACGGCAAGCTGATTGCTTACCCGATCGCTGTTGAAGCGTTATCGCTGATTTATAACAAAGATCTGCTGCCGA
ACCCGCCAAAAACCTGGGAAGAGATCCCGGCGCTGGATAAAGAACTGAAAGCGAAAGGTAAGAGCGCGCTGATGTTCAACCTGCAAGAACCGTACTTCACCTGGCCGCTGATTGCTGCTGACG
GGGGTTATGCGTTCAAGTATGAAAACGGCAAGTACGACATTAAAGACGTGGGCGTGGATAACGCTGGCGCGAAAGCGGGTCTGACCTTCCTGGTTGACCTGATTAAAAACAAACACATGAATG
CAGACACCGATTACTCCATCGCAGAAGCAGCCTTTAATAAAGGCGAAACAGCGATGACCATCAACGGCCCGTGGGCATGGTCCAACATCGACACCAGCAAAGTGAATTATGGTGTAACGGTAC
TGCCGACCTTCAAGGGTCAACCATCCAAACCGTTCGTTGGCGTGCTGAGCGCAGGTATTAACGCCGCCAGTCCGAACAAAGAGCTGGCAAAAGAGTTCCTCGAAAACTATCTGCTGACTGATG
AAGGTCTGGAAGCGGTTAATAAAGACAAACCGCTGGGTGCCGTAGCGCTGAAGTCTTACGAGGAAGAGTTGGTGAAAGATCCGCGTATTGCCGCCACTATGGAAAACGCCCAGAAAGGTGAAA
TCATGCCGAACATCCCGCAGATGTCCGCTTTCTGGTATGCCGTGCGTACTGCGGTGATCAACGCCGCCAGCGGTCGTCAGACTGTCGATGAAGCCCTGAAAGACGCGCAGACTCGCATTACCA
AAGGTGGCGGTAGCGAGAACTTATACTTTCAGGGTCATATGACGCTGACTGATTTGGAAACATGTGCCGAGGAGATCGCGACCGCTGCCCGCACATTAGCGCGTGATGGCCACAGCGGCGGCT
ACTCGGCGGGTTTGCCCGACCACTTACGTCCGGTGCAACGCACCTTGATCGCTAACGCGAGTCAGGTCTTGGCTCTCGCCTCGCAACCCGCTGATTTAGTGCGTCAGTTGGCGCTGTATAATC
AGTTACTGGCGTGTCTGCGGTGGTTAGGGGAATTTCAGGTATTAGCCTGCATCCCTCTGGATGAAAGCGTACCCTTCGAAGATGTTGCCGATATTGCAGGCGTTCCAGAATGCCGTTTACGTC
GCTTAGTTCGGCCATTATTTACCATCGGCTTTTTATGCGAACCGTCTCCGGGACACGTGGCTCACAGCGTGATGTCTAAACAGTTTGTGACCCAGCCGGCCCTGCTGGATGCGATCCTGTTCA
TGAGCGAGACCCTGGCGCCGAGCGCATCCGCTATGGGGACCCAGACTCGGCGCTTTGGCGCCTCGGTACCAGCGGAGGATTCGGCATGGAATATGGCGGTTGGTAGCGACTCCCCCTTTGCGG
CATGCTTGCAGCAGCGTCCGAAGGTGAAACGCCAATTGGGCGCGTACCTGAGCTACGTGAGTTCATCCATTGATGCGGGCGTGGAAGATACGCTGACGCGTATGAATTGGCAGAATCTGGGCA
TGGCGACCGTGGTACACGTTGGCGCACAGAGTCCGAGTCTGGTGGTGGCGTTAGCTCCTCAGTTCCCCAGTCTGCGCTTTCTCGTACAGACGGAAGCCAAAGCTGAGTCTGGAGGTCACCAGC
CTTGCCTGGACAATCACGGCATTTCCGCACTGAAATTGGCAAGCATCCCTCTGCATCTCCGCGCCCGCATCACGTGGGGGATGCATCTCTCGACTGCAACCCAGCCAGTGTTAGACGCAGCGG
TGTATTTGATCAGCATCCCATTTCCGTCTCCGCAGTCGCCGGCCATGGAAATCACGATGCGTGTTGCTCAAGCGCTTAAGGCGCATGTGGAAGTTCTGCGTAATAATAGCGACGCACGTCTGA
TCCTCACTTTACCAATGTCGAGCGCGACGCGCTCAATGGATGCAGCCGCGCGCGCGGCGGTGTCCCTGTCCGACCTGTCTCTGTTACAGCTGACTAACGGTGGTTCGCTGAACATGGGCGAAA
TTCGTGATCTCTTACGCAGTCGCAGCGATGGCCTGGTTGTCATGCGTGAAGTGCGTTCGCCTACCAATGCGGTTATTGCATTCGAGATCCAGTATCGGGTTGATAATGATGATAATCGTTATT
AACTCGAGCACCACCACCACCACCACTGAGATCCGGCTGCTAACAAAGCCCGAAAGGAAGCTGAGTTGGCTGCTGCCACCGCTGAGCAATAACTAGCATAACCCCTTGGGGCCTCTAAACGGG
TCTTGAGGGGTTTTTTGCTGAAAGGAGGAACTATATCCGGATTGGCGAATGGGACGCGCCCTGTAGCGGCGCATTAAGCGCGGCGGGTGTGGTGGTTACGCGCAGCGTGACCGCTACACTTGC
CAGCGCCCTAGCGCCCGCTCCTTTCGCTTTCTTCCCTTCCTTTCTCGCCACGTTCGCCGGCTTTCCCCGTCAAGCTCTAAATCGGGGGCTCCCTTTAGGGTTCCGATTTAGTGCTTTACGGCA
CCTCGACCCCAAAAAACTTGATTAGGGTGATGGTTCACGTAGTGGGCCATCGCCCTGATAGACGGTTTTTCGCCCTTTGACGTTGGAGTCCACGTTCTTTAATAGTGGACTCTTGTTCCAAAC
TGGAACAACACTCAACCCTATCTCGGTCTATTCTTTTGATTTATAAGGGATTTTGCCGATTTCGGCCTATTGGTTAAAAAATGAGCTGATTTAACAAAAATTTAACGCGAATTTTAACAAAAT
ATTAACGCTTACAATTTAGGTGGCACTTTTCGGGGAAATGTGCGCGGAACCCCTATTTGTTTATTTTTCTAAATACATTCAAATATGTATCCGCTCATGAGACAATAACCCTGATAAATGCTT
CAATAATATTGAAAAAGGAAGAGTATGAGTATTCAACATTTCCGTGTCGCCCTTATTCCCTTTTTTGCGGCATTTTGCCTTCCTGTTTTTGCTCACCCAGAAACGCTGGTGAAAGTAAAAGAT
GCTGAAGATCAGTTGGGTGCACGAGTGGGTTACATCGAACTGGATCTCAACAGCGGTAAGATCCTTGAGAGTTTTCGCCCCGAAGAACGTTTTCCAATGATGAGCACTTTTAAAGTTCTGCTA
TGTGGCGCGGTATTATCCCGTATTGACGCCGGGCAAGAGCAACTCGGTCGCCGCATACACTATTCTCAGAATGACTTGGTTGAGTACTCACCAGTCACAGAAAAGCATCTTACGGATGGCATG
ACAGTAAGAGAATTATGCAGTGCTGCCATAACCATGAGTGATAACACTGCGGCCAACTTACTTCTGACAACGATCGGAGGACCGAAGGAGCTAACCGCTTTTTTGCACAACATGGGGGATCAT
GTAACTCGCCTTGATCGTTGGGAACCGGAGCTGAATGAAGCCATACCAAACGACGAGCGTGACACCACGATGCCTGCAGCAATGGCAACAACGTTGCGCAAACTATTAACTGGCGAACTACTT
ACTCTAGCTTCCCGGCAACAATTAATAGACTGGATGGAGGCGGATAAAGTTGCAGGACCACTTCTGCGCTCGGCCCTTCCGGCTGGCTGGTTTATTGCTGATAAATCTGGAGCCGGTGAGCGT
GGGTCTCGCGGTATCATTGCAGCACTGGGGCCAGATGGTAAGCCCTCCCGTATCGTAGTTATCTACACGACGGGGAGTCAGGCAACTATGGATGAACGAAATAGACAGATCGCTGAGATAGGT
GCCTCACTGATTAAGCATTGGTAACTGTCAGACCAAGTTTACTCATATATACTTTAGATTGATTTAAAACTTCATTTTTAATTTAAAAGGATCTAGGTGAAGATCCTTTTTGATAATCTCATG
ACCAAAATCCCTTAACGTGAGTTTTCGTTCCACTGAGCGTCAGACCCCGTAGAAAAGATCAAAGGATCTTCTTGAGATCCTTTTTTTCTGCGCGTAATCTGCTGCTTGCAAACAAAAAAACCA
CCGCTACCAGCGGTGGTTTGTTTGCCGGATCAAGAGCTACCAACTCTTTTTCCGAAGGTAACTGGCTTCAGCAGAGCGCAGATACCAAATACTGTCCTTCTAGTGTAGCCGTAGTTAGGCCAC
CACTTCAAGAACTCTGTAGCACCGCCTACATACCTCGCTCTGCTAATCCTGTTACCAGTGGCTGCTGCCAGTGGCGATAAGTCGTGTCTTACCGGGTTGGACTCAAGACGATAGTTACCGGAT
AAGGCGCAGCGGTCGGGCTGAACGGGGGGTTCGTGCACACAGCCCAGCTTGGAGCGAACGACCTACACCGAACTGAGATACCTACAGCGTGAGCTATGAGAAAGCGCCACGCTTCCCGAAGGG
AGAAAGGCGGACAGGTATCCGGTAAGCGGCAGGGTCGGAACAGGAGAGCGCACGAGGGAGCTTCCAGGGGGAAACGCCTGGTATCTTTATAGTCCTGTCGGGTTTCGCCACCTCTGACTTGAG
CGTCGATTTTTGTGATGCTCGTCAGGGGGGCGGAGCCTATGGAAAAACGCCAGCAACGCGGCCTTTTTACGGTTCCTGGCCTTTTGCTGGCCTTTTGCTCACATGTTCTTTCCTGCGTTATCC
CCTGATTCTGTGGATAACCGTATTACCGCCTTTGAGTGAGCTGATACCGCTCGCCGCAGCCGAACGACCGAGCGCAGCGAGTCAGTGAGCGAGGAAGCGGAAGAGCGCCTGATGCGGTATTTT
CTCCTTACGCATCTGTGCGGTATTTCACACCGCAATGGTGCACTCTCAGTACAATCTGCTCTGATGCCGCATAGTTAAGCCAGTATACACTCCGCTATCGCTACGTGACTGGGTCATGGCTGC
GCCCCGACACCCGCCAACACCCGCTGACGCGCCCTGACGGGCTTGTCTGCTCCCGGCATCCGCTTACAGACAAGCTGTGACCGTCTCCGGGAGCTGCATGTGTCAGAGGTTTTCACCGTCATC
ACCGAAACGCGCGAGGCAGCTGCGGTAAAGCTCATCAGCGTGGTCGTGAAGCGATTCACAGATGTCTGCCTGTTCATCCGCGTCCAGCTCGTTGAGTTTCTCCAGAAGCGTTAATGTCTGGCT
TCTGATAAAGCGGGCCATGTTAAGGGCGGTTTTTTCCTGTTTGGTCACTGATGCCTCCGTGTAAGGGGGATTTCTGTTCATGGGGGTAATGATACCGATGAAACGAGAGAGGATGCTCACGAT
ACGGGTTACTGATGATGAACATGCCCGGTTACTGGAACGTTGTGAGGGTAAACAACTGGCGGTATGGATGCGGCGGGACCAGAGAAAAATCACTCAGGGTCAATGCCAGCGCTTCGTTAATAC
AGATGTAGGTGTTCCACAGGGTAGCCAGCAGCATCCTGCGATGCAGATCCGGAACATAATGGTGCAGGGCGCTGACTTCCGCGTTTCCAGACTTTACGAAACACGGAAACCGAAGACCATTCA
TGTTGTTGCTCAGGTCGCAGACGTTTTGCAGCAGCAGTCGCTTCACGTTCGCTCGCGTATCGGTGATTCATTCTGCTAACCAGTAAGGCAACCCCGCCAGCCTAGCCGGGTCCTCAACGACAG
GAGCACGATCATGCGCACCCGTGGGGCCGCCATGCCGGCGATAATGGCCTGCTTCTCGCCGAAACGTTTGGTGGCGGGACCAGTGACGAAGGCTTGAGCGAGGGCGTGCAAGATTCCGAATAC
CGCAAGCGACAGGCCGATCATCGTCGCGCTCCAGCGAAAGCGGTCCTCGCCGAAAATGACCCAGAGCGCTGCCGGCACCTGTCCTACGAGTTGCATGATAAAGAAGACAGTCATAAGTGCGGC
GACGATAGTCATGCCCCGCGCCCACCGGAAGGAGCTGACTGGGTTGAAGGCTCTCAAGGGCATCGGTCGAGATCCCGGTGCCTAATGAGTGAGCTAACTTACATTAATTGCGTTGCGCTCACT
GCCCGCTTTCCAGTCGGGAAACCTGTCGTGCCAGCTGCATTAATGAATCGGCCAACGCGCGGGGAGAGGCGGTTTGCGTATTGGGCGCCAGGGTGGTTTTTCTTTTCACCAGTGAGACGGGCA
ACAGCTGATTGCCCTTCACCGCCTGGCCCTGAGAGAGTTGCAGCAAGCGGTCCACGCTGGTTTGCCCCAGCAGGCGAAAATCCTGTTTGATGGTGGTTAACGGCGGGATATAACATGAGCTGT
CTTCGGTATCGTCGTATCCCACTACCGAGATATCCGCACCAACGCGCAGCCCGGACTCGGTAATGGCGCGCATTGCGCCCAGCGCCATCTGATCGTTGGCAACCAGCATCGCAGTGGGAACGA
TGCCCTCATTCAGCATTTGCATGGTTTGTTGAAAACCGGACATGGCACTCCAGTCGCCTTCCCGTTCCGCTATCGGCTGAATTTGATTGCGAGTGAGATATTTATGCCAGCCAGCCAGACGCA
GACGCGCCGAGACAGAACTTAATGGGCCCGCTAACAGCGCGATTTGCTGGTGACCCAATGCGACCAGATGCTCCACGCCCAGTCGCGTACCGTCTTCATGGGAGAAAATAATACTGTTGATGG
GTGTCTGGTCAGAGACATCAAGAAATAACGCCGGAACATTAGTGCAGGCAGCTTCCACAGCAATGGCATCCTGGTCATCCAGCGGATAGTTAATGATCAGCCCACTGACGCGTTGCGCGAGAA
GATTGTGCACCGCCGCTTTACAGGCTTCGACGCCGCTTCGTTCTACCATCGACACCACCACGCTGGCACCCAGTTGATCGGCGCGAGATTTAATCGCCGCGACAATTTGCGACGGCGCGTGCA
GGGCCAGACTGGAGGTGGCAACGCCAATCAGCAACGACTGTTTGCCCGCCAGTTGTTGTGCCACGCGGTTGGGAATGTAATTCAGCTCCGCCATCGCCGCTTCCACTTTTTCCCGCGTTTTCG
CAGAAACGTGGCTGGCCTGGTTCACCACGCGGGAAACGGTCTGATAAGAGACACCGGCATACTCTGCGACATCGTATAACGTTACTGGTTTCACATTCACCACCCTGAATTGACTCTCTTCCG
GGCGCTATCATGCCATACCGCGAAAGGTTTTGCGCCATTCGATGGTGTCCGGGATCTCGACGCTCTCCCTTATGCGACTCCTGCATTAGGAAGCAGCCCAGTAGTAGGTTGAGGCCGTTGAGC
ACCGCCGCCGCAAGGAATGGTGCATGCAAGGAGATGGCGCCCAACAGTCCCCCGGCCACGGGGCCTGCCACCATACCCACGCCGAAACAAGCGCTCATGAGCCCGAAGTGGCGAGCCCGATCT
TCCCCATCGGTGATGTCGGCGATATAGGCGCCAGCAACCGCACCTGTGGCGCCGGTGATGCCGGCCACGATGCGTCCGGCGTAGAGGATCGAGATCT

Figure S8. Sequence of plasmid pAM073. The plasmid was used to express *Aspergillus flavus* AflS fused with maltose binding protein [AflS(MBP)].

>pAM074
CGATCCCGCGAAATTAATACGACTCACTATAGGGGAATTGTGAGCGGATAACAATTCCCCTCTAGAAATAATTTTGTTTAACTTTAAGAAGGAGATATACCATGGGGAGTCACC
ATCACCACCACCACGAAGAAGGTAAACTGGTAATCTGGATTAACGGCGATAAAGGCTATAACGGTCTCGCTGAAGTCGGTAAGAAATTCGAGAAAGATACCGGAATTAAAGTCA
CCGTTGAGCATCCGGATAAACTGGAAGAGAAATTCCCACAGGTTGCGGCAACTGGCGATGGCCCTGACATTATCTTCTGGGCACACGACCGCTTTGGTGGCTACGCTCAATCTG
GCCTGTTGGCTGAAATCACCCCGGACAAAGCGTTCCAGGACAAGCTGTATCCGTTTACCTGGGATGCCGTACGTTACAACGGCAAGCTGATTGCTTACCCGATCGCTGTTGAAG
CGTTATCGCTGATTTATAACAAAGATCTGCTGCCGAACCCGCCAAAAACCTGGGAAGAGATCCCGGCGCTGGATAAAGAACTGAAAGCGAAAGGTAAGAGCGCGCTGATGTTCA
ACCTGCAAGAACCGTACTTCACCTGGCCGCTGATTGCTGCTGACGGGGGTTATGCGTTCAAGTATGAAAACGGCAAGTACGACATTAAAGACGTGGGCGTGGATAACGCTGGCG
CGAAAGCGGGTCTGACCTTCCTGGTTGACCTGATTAAAAACAAACACATGAATGCAGACACCGATTACTCCATCGCAGAAGCAGCCTTTAATAAAGGCGAAACAGCGATGACCA
TCAACGGCCCGTGGGCATGGTCCAACATCGACACCAGCAAAGTGAATTATGGTGTAACGGTACTGCCGACCTTCAAGGGTCAACCATCCAAACCGTTCGTTGGCGTGCTGAGCG
CAGGTATTAACGCCGCCAGTCCGAACAAAGAGCTGGCAAAAGAGTTCCTCGAAAACTATCTGCTGACTGATGAAGGTCTGGAAGCGGTTAATAAAGACAAACCGCTGGGTGCCG
TAGCGCTGAAGTCTTACGAGGAAGAGTTGGTGAAAGATCCGCGTATTGCCGCCACTATGGAAAACGCCCAGAAAGGTGAAATCATGCCGAACATCCCGCAGATGTCCGCTTTCT
GGTATGCCGTGCGTACTGCGGTGATCAACGCCGCCAGCGGTCGTCAGACTGTCGATGAAGCCCTGAAAGACGCGCAGACTCGCATTACCAAAGGTGGCGGTAGCTAACTCGAGC
ACCACCACCACCACCACTGAGATCCGGCTGCTAACAAAGCCCGAAAGGAAGCTGAGTTGGCTGCTGCCACCGCTGAGCAATAACTAGCATAACCCCTTGGGGCCTCTAAACGGG
TCTTGAGGGGTTTTTTGCTGAAAGGAGGAACTATATCCGGATTGGCGAATGGGACGCGCCCTGTAGCGGCGCATTAAGCGCGGCGGGTGTGGTGGTTACGCGCAGCGTGACCGC
TACACTTGCCAGCGCCCTAGCGCCCGCTCCTTTCGCTTTCTTCCCTTCCTTTCTCGCCACGTTCGCCGGCTTTCCCCGTCAAGCTCTAAATCGGGGGCTCCCTTTAGGGTTCCG
ATTTAGTGCTTTACGGCACCTCGACCCCAAAAAACTTGATTAGGGTGATGGTTCACGTAGTGGGCCATCGCCCTGATAGACGGTTTTTCGCCCTTTGACGTTGGAGTCCACGTT
CTTTAATAGTGGACTCTTGTTCCAAACTGGAACAACACTCAACCCTATCTCGGTCTATTCTTTTGATTTATAAGGGATTTTGCCGATTTCGGCCTATTGGTTAAAAAATGAGCT
GATTTAACAAAAATTTAACGCGAATTTTAACAAAATATTAACGCTTACAATTTAGGTGGCACTTTTCGGGGAAATGTGCGCGGAACCCCTATTTGTTTATTTTTCTAAATACAT
TCAAATATGTATCCGCTCATGAGACAATAACCCTGATAAATGCTTCAATAATATTGAAAAAGGAAGAGTATGAGTATTCAACATTTCCGTGTCGCCCTTATTCCCTTTTTTGCG
GCATTTTGCCTTCCTGTTTTTGCTCACCCAGAAACGCTGGTGAAAGTAAAAGATGCTGAAGATCAGTTGGGTGCACGAGTGGGTTACATCGAACTGGATCTCAACAGCGGTAAG
ATCCTTGAGAGTTTTCGCCCCGAAGAACGTTTTCCAATGATGAGCACTTTTAAAGTTCTGCTATGTGGCGCGGTATTATCCCGTATTGACGCCGGGCAAGAGCAACTCGGTCGC
CGCATACACTATTCTCAGAATGACTTGGTTGAGTACTCACCAGTCACAGAAAAGCATCTTACGGATGGCATGACAGTAAGAGAATTATGCAGTGCTGCCATAACCATGAGTGAT
AACACTGCGGCCAACTTACTTCTGACAACGATCGGAGGACCGAAGGAGCTAACCGCTTTTTTGCACAACATGGGGGATCATGTAACTCGCCTTGATCGTTGGGAACCGGAGCTG
AATGAAGCCATACCAAACGACGAGCGTGACACCACGATGCCTGCAGCAATGGCAACAACGTTGCGCAAACTATTAACTGGCGAACTACTTACTCTAGCTTCCCGGCAACAATTA
ATAGACTGGATGGAGGCGGATAAAGTTGCAGGACCACTTCTGCGCTCGGCCCTTCCGGCTGGCTGGTTTATTGCTGATAAATCTGGAGCCGGTGAGCGTGGGTCTCGCGGTATC
ATTGCAGCACTGGGGCCAGATGGTAAGCCCTCCCGTATCGTAGTTATCTACACGACGGGGAGTCAGGCAACTATGGATGAACGAAATAGACAGATCGCTGAGATAGGTGCCTCA
CTGATTAAGCATTGGTAACTGTCAGACCAAGTTTACTCATATATACTTTAGATTGATTTAAAACTTCATTTTTAATTTAAAAGGATCTAGGTGAAGATCCTTTTTGATAATCTC
ATGACCAAAATCCCTTAACGTGAGTTTTCGTTCCACTGAGCGTCAGACCCCGTAGAAAAGATCAAAGGATCTTCTTGAGATCCTTTTTTTCTGCGCGTAATCTGCTGCTTGCAA
ACAAAAAAACCACCGCTACCAGCGGTGGTTTGTTTGCCGGATCAAGAGCTACCAACTCTTTTTCCGAAGGTAACTGGCTTCAGCAGAGCGCAGATACCAAATACTGTCCTTCTA
GTGTAGCCGTAGTTAGGCCACCACTTCAAGAACTCTGTAGCACCGCCTACATACCTCGCTCTGCTAATCCTGTTACCAGTGGCTGCTGCCAGTGGCGATAAGTCGTGTCTTACC
GGGTTGGACTCAAGACGATAGTTACCGGATAAGGCGCAGCGGTCGGGCTGAACGGGGGGTTCGTGCACACAGCCCAGCTTGGAGCGAACGACCTACACCGAACTGAGATACCTA
CAGCGTGAGCTATGAGAAAGCGCCACGCTTCCCGAAGGGAGAAAGGCGGACAGGTATCCGGTAAGCGGCAGGGTCGGAACAGGAGAGCGCACGAGGGAGCTTCCAGGGGGAAAC
GCCTGGTATCTTTATAGTCCTGTCGGGTTTCGCCACCTCTGACTTGAGCGTCGATTTTTGTGATGCTCGTCAGGGGGGCGGAGCCTATGGAAAAACGCCAGCAACGCGGCCTTT
TTACGGTTCCTGGCCTTTTGCTGGCCTTTTGCTCACATGTTCTTTCCTGCGTTATCCCCTGATTCTGTGGATAACCGTATTACCGCCTTTGAGTGAGCTGATACCGCTCGCCGC
AGCCGAACGACCGAGCGCAGCGAGTCAGTGAGCGAGGAAGCGGAAGAGCGCCTGATGCGGTATTTTCTCCTTACGCATCTGTGCGGTATTTCACACCGCAATGGTGCACTCTCA
GTACAATCTGCTCTGATGCCGCATAGTTAAGCCAGTATACACTCCGCTATCGCTACGTGACTGGGTCATGGCTGCGCCCCGACACCCGCCAACACCCGCTGACGCGCCCTGACG
GGCTTGTCTGCTCCCGGCATCCGCTTACAGACAAGCTGTGACCGTCTCCGGGAGCTGCATGTGTCAGAGGTTTTCACCGTCATCACCGAAACGCGCGAGGCAGCTGCGGTAAAG
CTCATCAGCGTGGTCGTGAAGCGATTCACAGATGTCTGCCTGTTCATCCGCGTCCAGCTCGTTGAGTTTCTCCAGAAGCGTTAATGTCTGGCTTCTGATAAAGCGGGCCATGTT
AAGGGCGGTTTTTTCCTGTTTGGTCACTGATGCCTCCGTGTAAGGGGGATTTCTGTTCATGGGGGTAATGATACCGATGAAACGAGAGAGGATGCTCACGATACGGGTTACTGA
TGATGAACATGCCCGGTTACTGGAACGTTGTGAGGGTAAACAACTGGCGGTATGGATGCGGCGGGACCAGAGAAAAATCACTCAGGGTCAATGCCAGCGCTTCGTTAATACAGA
TGTAGGTGTTCCACAGGGTAGCCAGCAGCATCCTGCGATGCAGATCCGGAACATAATGGTGCAGGGCGCTGACTTCCGCGTTTCCAGACTTTACGAAACACGGAAACCGAAGAC
CATTCATGTTGTTGCTCAGGTCGCAGACGTTTTGCAGCAGCAGTCGCTTCACGTTCGCTCGCGTATCGGTGATTCATTCTGCTAACCAGTAAGGCAACCCCGCCAGCCTAGCCG
GGTCCTCAACGACAGGAGCACGATCATGCGCACCCGTGGGGCCGCCATGCCGGCGATAATGGCCTGCTTCTCGCCGAAACGTTTGGTGGCGGGACCAGTGACGAAGGCTTGAGC
GAGGGCGTGCAAGATTCCGAATACCGCAAGCGACAGGCCGATCATCGTCGCGCTCCAGCGAAAGCGGTCCTCGCCGAAAATGACCCAGAGCGCTGCCGGCACCTGTCCTACGAG
TTGCATGATAAAGAAGACAGTCATAAGTGCGGCGACGATAGTCATGCCCCGCGCCCACCGGAAGGAGCTGACTGGGTTGAAGGCTCTCAAGGGCATCGGTCGAGATCCCGGTGC
CTAATGAGTGAGCTAACTTACATTAATTGCGTTGCGCTCACTGCCCGCTTTCCAGTCGGGAAACCTGTCGTGCCAGCTGCATTAATGAATCGGCCAACGCGCGGGGAGAGGCGG
TTTGCGTATTGGGCGCCAGGGTGGTTTTTCTTTTCACCAGTGAGACGGGCAACAGCTGATTGCCCTTCACCGCCTGGCCCTGAGAGAGTTGCAGCAAGCGGTCCACGCTGGTTT
GCCCCAGCAGGCGAAAATCCTGTTTGATGGTGGTTAACGGCGGGATATAACATGAGCTGTCTTCGGTATCGTCGTATCCCACTACCGAGATATCCGCACCAACGCGCAGCCCGG
ACTCGGTAATGGCGCGCATTGCGCCCAGCGCCATCTGATCGTTGGCAACCAGCATCGCAGTGGGAACGATGCCCTCATTCAGCATTTGCATGGTTTGTTGAAAACCGGACATGG
CACTCCAGTCGCCTTCCCGTTCCGCTATCGGCTGAATTTGATTGCGAGTGAGATATTTATGCCAGCCAGCCAGACGCAGACGCGCCGAGACAGAACTTAATGGGCCCGCTAACA
GCGCGATTTGCTGGTGACCCAATGCGACCAGATGCTCCACGCCCAGTCGCGTACCGTCTTCATGGGAGAAAATAATACTGTTGATGGGTGTCTGGTCAGAGACATCAAGAAATA
ACGCCGGAACATTAGTGCAGGCAGCTTCCACAGCAATGGCATCCTGGTCATCCAGCGGATAGTTAATGATCAGCCCACTGACGCGTTGCGCGAGAAGATTGTGCACCGCCGCTT
TACAGGCTTCGACGCCGCTTCGTTCTACCATCGACACCACCACGCTGGCACCCAGTTGATCGGCGCGAGATTTAATCGCCGCGACAATTTGCGACGGCGCGTGCAGGGCCAGAC
TGGAGGTGGCAACGCCAATCAGCAACGACTGTTTGCCCGCCAGTTGTTGTGCCACGCGGTTGGGAATGTAATTCAGCTCCGCCATCGCCGCTTCCACTTTTTCCCGCGTTTTCG
CAGAAACGTGGCTGGCCTGGTTCACCACGCGGGAAACGGTCTGATAAGAGACACCGGCATACTCTGCGACATCGTATAACGTTACTGGTTTCACATTCACCACCCTGAATTGAC
TCTCTTCCGGGCGCTATCATGCCATACCGCGAAAGGTTTTGCGCCATTCGATGGTGTCCGGGATCTCGACGCTCTCCCTTATGCGACTCCTGCATTAGGAAGCAGCCCAGTAGT
AGGTTGAGGCCGTTGAGCACCGCCGCCGCAAGGAATGGTGCATGCAAGGAGATGGCGCCCAACAGTCCCCCGGCCACGGGGCCTGCCACCATACCCACGCCGAAACAAGCGCTC
ATGAGCCCGAAGTGGCGAGCCCGATCTTCCCCATCGGTGATGTCGGCGATATAGGCGCCAGCAACCGCACCTGTGGCGCCGGTGATGCCGGCCACGATGCGTCCGGCGTAGAGG
ATCGAGATCT

Figure S9. Sequences of plasmid pAM074. The plasmid was used to express maltose binding protein (MBP)